# ORBIT DETERMINATION IN THE PRESENCE OF GRAVITY MODEL ERRORS

B. E. Schutz, et al

Texas University

Prepared for:

Air Force Office of Scientific Research

August 1972

# ORBIT DETERMINATION IN THE PRESENCE OF GRAVITY MODEL ERRORS

B. E. Schutz, B. D. Tapley, and P. E. Connolly
The University of Texas at Austin



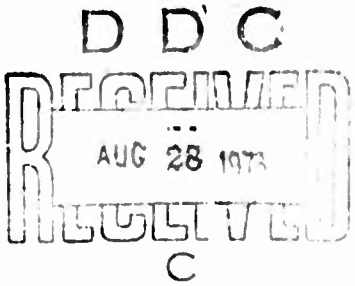




Symposium on Earth Gravity Models
St. Louis, Missouri
August 16-18, 1972

# ORBIT DETERMINATION IN THE PRESENCE OF GRAVITY MODEL ERRORS[#]

B. E. Schutz[1], B. D. Tapley[2], and P. E. Connolly[3]
The University of Texas at Austin

## Abstract

The precise determination of a satellite's position is of prime importance in satellite geodesy and in the use of satellites in studying geodynamics. It is not possible, however, to obtain a precise estimate of the satellite's position if sufficiently large errors exist in the gravity model. In this investigation, the application of a dynamic model compensation method to the problem of estimating the motion of a near-earth satellite in the presence of gravity model errors is described. Based on numerical results obtained in a computer simulation, it is concluded that the algorithm will yield an accurate estimate of the state in the presence of gravity model errors. The effects of the observation type and accuracy, station location and observation batch size on the accuracy of the orbit determination procedure are considered. Finally, it is shown that in addition to an accurate estimate of the position and velocity, the method can be used to obtain an accurate estimate of the unmodeled acceleration components.

---

[1]Assistant Professor, Department of Aerospace Engineering and Engineering Mechanics, The University of Texas at Austin
[2]Professor and Chairman, Department of Aerospace Engineering and Engineering Mechanics, The University of Texas at Austin
[3]Research Assistant, now assigned to Aerospace Defense Command, Laredo Air Force Base, Laredo, Texas
[#]This investigation was supported by AFOSR Grant No. 72-2233.

Security Classification

**DOCUMENT CONTROL DATA - R & D**

*(Security classification of title, body of abstract and indexing annotation must be entered when the overall report is classified)*

| 1. ORIGINATING ACTIVITY (Corporate author) | 2a. REPORT SECURITY CLASSIFICATION |
|---|---|
| University of Texas at Austin<br>Dept of Aerospace Engineering & Engineering Mechanics<br>Austin, Texas 78712 | UNCLASSIFIED<br>2b. GROUP |

3. REPORT TITLE

ORBIT DETERMINATION IN THE PRESENCE OF GRAVITY MODEL ERRORS

4. DESCRIPTIVE NOTES (Type of report and inclusive dates)

Scientific Interim

5. AUTHOR(S) (First name, middle initial, last name)

B. E. Schutz
B. D. Tapley
P. E. Connolly

| 6. REPORT DATE | 7a. TOTAL NO OF PAGES | 7b. NO OF REFS |
|---|---|---|
| August 1972 | 40 41 | 18 |

| 8a. CONTRACT OR GRANT NO | 9a. ORIGINATOR'S REPORT NUMBER(S) |
|---|---|
| AFOSR 72-2233<br>b. PROJECT NO 9769<br>c. 61102F<br>d. 681304 | 9b. OTHER REPORT NO(S) (Any other numbers that may be assigned this report)<br>AFOSR - TR - 73 - 1439 |

10. DISTRIBUTION STATEMENT

Approved for public release; distribution unlimited.

| 11. SUPPLEMENTARY NOTES | 12. SPONSORING MILITARY ACTIVITY |
|---|---|
| PROCEEDINGS<br>Symposium on Earth Gravity Models, St. Louis, Missouri, 16-18 August 1972 | Air Force Office of Scientific Rsch (NM)<br>1400 Wilson Blvd<br>Arlington, Virginia 22209 |

13. ABSTRACT

The precise determination of a satellite's position is of prime importance in satellite geodesy and in the use of satellites in studying geodynamics. It is not possible, however, to obtain a precise estimate of the satellite's position if sufficiently large errors exist in the gravity model. In this investigation, the application of a dynamic model compensation method to the problem of estimating the motion of a near-earth satellite in the presence of gravity model errors is described XXXX Based on numerical results obtained in a computer simulation, it is concluded that the algorithm will yield an accurate estimate of the state in the presence of gravity model errors. The effects of the observation type and accuracy, station location and observation batch size on the accuracy of the orbit determination procedure are considered. Finally, it is shown that in addition to an accurate estimate of the position and velocity, the method can be used to obtain an accurate estimate of the unmodeled acceleration components.

DD FORM 1 NOV 1473

Security Classification

## Introduction

With the recent improvements and refinements in the instruments used in the observations of near-earth satellites, measurements of range and range-rate with precision of less than one meter and one centimeter per second, respectively, are a reality. Such precise observations have potential for determination of the satellite's state, namely, position and velocity, to the precision necessary for geodesy and geodynamics studies.

A determination of the satellite's state commensurate with the observation accuracy using the classical batch processor (least squares) or the sequential filtering method is dependent on the accuracy of the tracking station locations and the model of the dynamical system. Such dependence on the model of the dynamical system is demonstrated by Smith, Kolenkiewicz, and Dunn (1971), Marsh and Douglas (1971), and Yionoulis, Heuring, and Guier (1972). Uncertainties in the geopotential, particularly resonant coefficients in some cases, are an important error source. Additional errors often occur in the atmospheric resistance modeling. The discrepancy between the true motion and the modeled motion often limit the usefulness of the orbit determination results, both from the point of view of using the estimates for navigation purposes as well as using them for scientific purposes.

The effect of gravity model errors on the accuracy of batch-type orbit determination methods was observed also in processing the Lunar Orbiter range-rate observations. Observation residuals were obtained which clearly showed a periodic variation with an amplitude larger than the observation noise. The work of Muller and Sjogren (1971) and Sjogren and Muller (1971) resulted in a mascon representation for the gravity anomalies.

A somewhat different approach was taken by Tapley and Ingram (1971) and Ingram and Tapley (1971) using a sequential estimation procedure which compensated for the model errors. In this approach, referred to as the Dynamic Model Compensation

(DMC) method, the model errors are assumed to consist of a time correlated component and a purely random component and are approximated by a first-order Gauss-Markov process. Application of the DMC method to the lunar orbit phase of the Apollo 10 and 11 spacecraft showed that (1) the DMC method obtained observation residuals within the observation noise level and (2) provided estimates of the acceleration due to the model error which could be correlated with the surface mass anomalies described by Sjogren and Muller (1971). Additional applications of the DMC method have been made by Tapley and Schutz (1972) to the problem of estimating unmodeled forces due to errors in the lunar potential. In addition, Connolly (1972) considered application of the method to the orbit determination problem of a near-earth satellite.

Other applications of statistical models have been explored by Shaw, Paul, and Henrikson (1969) for use in inertial navigation systems. Shaw et al. used statistical models for the vertical deflection from gravity anomaly models. More recently, Kasper (1971) and Jordan (1972) have utilized second-order Gauss-Markov processes to represent the gravity anomaly.

In this investigation, the question of how accurately both the state of the satellite and the acceleration due to model errors can be estimated for a near-earth satellite is considered. A near-earth orbit of 1000 km inclined at 42° is assumed for the study. In the investigation, computer simulation techniques were used to investigate the behavior of the DMC method as applied to the orbit determination problem of a near-earth satellite. In this study, the model errors were assumed to arise from an incomplete description of the geopotential. Two sets of simulated observations were generated, each resulting from a different method of simulating gravity model errors. It is shown that state estimates can be obtained which reduce the observation residuals to within the apriori observation accuracy and that the methods can be used to obtain an accurate estimate of

the accelerations due to gravity model error. The influence of observation accuracy, the magnitude of the model error, and the number of tracking stations on the accuracy with which the acceleration due to the model error can be estimated is discussed.

The Estimation Procedure

The equations which describe the motion of an earth satellite can be expressed by the following system of first-order equations:

$$\dot{r} = v \quad , \quad \dot{v} = a_c + a_p + m(t) \tag{1}$$

where r is a three-vector of position components, v is a three-vector of velocity components, $a_c$ is the acceleration due to the central body, $a_p$ is the modeled acceleration due to other sources, gravitational or otherwise, and m represents the acceleration due to incorrect modeling in $a_c$ and $a_p$. The term m(t) will be referred to as the "unmodeled acceleration".

The three-vector m(t) represents the effects of all accelerations not accounted for in the mathematical model used to describe the motion of the satellite. In this discussion, m(t) is approximated as a first-order Gauss-Markov process, $\varepsilon(t)$, which satisfies the following vector differential equation

$$\dot{\varepsilon}(t) = B\varepsilon(t) + u(t) \tag{2}$$

where u(t) is a three-vector of Gaussian noise whose components are assumed to be described by the statistics:

$$E[u(t)] = 0 \quad , \quad E[u(t)u^T(\tau)] = q(t)\delta(t-\tau) \tag{3}$$

where q(t) is a 3 x 3 positive definite matrix. The coefficient matrix B is defined by the components $B_{ij} = \frac{1}{T_i}\delta_{ij}$ where $T_i$, the time-correlation coefficients, are assumed to be unknown parameters whose values are to be determined during the estimation process. The state vector is then defined to be

$$X^T = [r^T : v^T : \varepsilon^T : T^T] \quad .$$

Then the differential equations of state become

$$\dot{X} = \begin{bmatrix} v \\ a_c + a_p + \epsilon \\ B\epsilon + u \\ 0 \end{bmatrix} \tag{4}$$

with the initial conditions $X(t_o) = X_o$.

In the following discussion, it is assumed that the observation noise, $v_i$, satisfies the following conditions:

$$E[v_i] = 0 \quad , \quad E[v_i v_j^T] = R_i \delta_{ij} \quad , \quad E[v_i X_j^T] = 0 \quad , \tag{5}$$

where E[ ] is the expected value operator. Further, the observations are related to the state by the relation

$$y_i = G(x_i, t_i) + v_i \tag{6}$$

where $G(X_i, t)$ is some nonlinear function of the state.

The problem considered then is posed as follows: Given the relation for propagating the state, Eq. (4); the observation state relation, Eq. (6); a sequence of observations $Y_i$, i = 1, ..., k; the statistics on the state noise, Eq. (3); and the observation noise, Eq. (5), determine the best estimate of the state in the minimum variance sense, $\hat{X}_k$, at the time $t_k$. Under these conditions the estimate can be obtained using the following algorithm (Jazwinski, 1969):

$$\begin{aligned} \bar{X}_k &= \theta(\hat{X}_{k-1}, t_{k-1}, t_k) \\ \bar{P}_k &= \Phi(t_k, t_{k-1}) P_{k-1} \Phi^T(t_k, t_{k-1}) + Q_{k-1} \\ K_k &= \bar{P}_k H_k^T [H_k \bar{P}_k H_k^T + R_k]^{-1} \\ \hat{X}_k &= \bar{X}_k + K_k [Y_k - G(\bar{X}_k, t_k)] \\ P_k &= [I - K_k H_k] \bar{P}_k \end{aligned} \tag{7}$$

where $H_k = [\partial G / \partial X_k]^*$, $\bar{X}_k = E[X_k \mid Y_1, \ldots, Y_{k-1}]$ and $\hat{X}_k = E[X_k \mid Y_1, \ldots, Y_k]$.

The covariance matrices $\bar{P}_k$ and $P_k$ are associated with the state estimates $\bar{X}_k$ and $\hat{X}_k$, respectively. The state transition matrix, $\Phi(t_k, t_{k-1})$ satisfies the following differential equation

$$\dot{\Phi}(t, t_k) = A(t) \quad \Phi(t, t_k) \; ; \; \Phi(t, t_k) = I \tag{8}$$

where $A(t) = [\partial F/\partial X]^*$. The symbol $[]^*$ indicates that the quantity in the bracket is evaluated on the nominal solution, $\bar{X}(t) = \theta(\hat{X}_{k-1}, t_{k-1}, t)$, $t_k \leq t$, that is, the solution obtained by integrating Eqs. (4) with the condition $X^*(t_{k-1}) = \hat{X}_{k-1}$ and $u^* = E[u(t)] = 0$. The algorithm given by Eqs. (7) and (8) is the extended form of the linear sequential estimator, or the Kalman-Bucy filter, as discussed by Jazwinski (1969). The covariance matrix $P_k$ is associated with the best estimate of $X_k$ based on k-observations while $\bar{P}_k$ is the covariance matrix associated with the best estimate of $x_k$ based on (k-1) observations.

It should be recalled that the estimate $\hat{X}_k$, includes an estimate at the time, $t_k$, of the components of the position, the velocity, the unmodeled acceleration $\bar{\varepsilon}(t)$ and the correlation coefficients, $T_x$, $T_y$, and $T_z$. The algorithm requires apriori or "initial" estimates of each of these quantities as well as the apriori covariance matrices, $P_o$, $Q_i$, and $R_i$, associated with the initial state and with the state and the observation noise, respectively. The development of the algorithm and the computational procedure required to implement the algorithm are discussed in greater detail by Ingram (1971).

The following section describes the generation of the observations used in the estimation procedure and discusses the simulation of the gravity model errors.

Generation of the Simulated Observations

The simulated observations are generated by the integration of the system of equations

$$\dot{r}_T = v_T \quad , \quad \dot{v}_T = a_m + m \tag{9}$$

where $r_T$ is a three-vector of the true position components, $v_T$ is a three-vector of the true velocity components, $a_m$ represents the terms modeled in the estimation algorithm, and m represents the terms not directly included in the estimation differential equations. The term m represents a model error in the estimation procedure. To simulate model errors, two forms for m were used. First, m is assumed to represent the acceleration due to a point mass on the surface of the earth and close to the satellite's ground track. The term $a_m$ includes all of the zonal harmonics up to the sixth degree as well as the tesseral and sectorial harmonics up to fourth-order and the lunar gravitational effect. In the second form, $a_m$ includes $J_2$ and the lunar effect, whereas m contained the geopotential terms up to sixth degree in the zonal harmonics and all other terms to the fourth order.

Integration of Eq. (9) yields a solution for the motion of the satellite used in generating observations. The computer program ascertains which tracking stations can observe the satellite and an observation (either range, azimuth, elevation, range-rate or any combination) is computed. These observations are then corrupted by adding the quantity, $\sigma\lambda$, where $\sigma$ is the standard deviation of the observation noise and $\lambda$ is a Gaussian distributed random variable with zero mean.

The numerical integration is performed using the Runge-Kutta methods formulated by Fehlberg (1968). As implemented in the simulation program, two different order integrators can be used. For periods when the satellite cannot be seen by any of the tracking stations, the Runge-Kutta-Fehlberg 7(8) is used with a variable stepsize control. During periods in which observations are being generated, a fixed step is used to comply with a fixed observation interval.

This interval is normally small enough to allow use of a lower order integrator, namely, the Runge-Kutta-Fehlberg 4(5). If the observation interval results in a stepsize which is too large and the 4(5) is inadequate for maintaining accuracy, the 7(8) method can be used.

Data

The estimation program requires the numerical integration of Eq. (4) and Eq. (8), whereas the observation generation program requires the integration of Eq. (9). The state vector of Eq. (4) consists of 12 elements, the state transition matrix consists of 144 elements, and Eq. (8) consists of six elements. Eq. (8), $\dot{\Phi}$, can, however, be reduced to a lower order by noting that a number of elements are zero.

The initial conditions for Eq. (4) and Eq. (9) used in the simulation are shown in Table I. A rectangular coordinate system is used in which X and Y are in the equatorial plane and Z is along the polar axis. The ground track of the satellite is shown in Fig. 1 where the semi-major axis of the satellite orbit is 7,507,000 meters, the eccentricity is .025, and the inclination is 41.2°. These orbital elements closely approximate those of the Beacon Explorer C (BE-C) spacecraft (Kolenkiewicz, 1972).

The assumed tracking station locations used in the simulations are shown in Table II. In general, the observations from horizon-to-horizon of the tracking station are used in the estimation process. However, several cases were examined in which a 25° elevation constraint was imposed. These results are discussed in a later section. The period of time during which each station can observe the satellite is shown also in Figure II. Although Figure II shows 15 stations, not all stations are used.

The geopotential coefficients used were given by Melbourne, et al (1968). Since these coefficients were being used to simulate a gravity model error, a more accurate set such as those determined by Gaposchkin and Lambeck (1970) was not required.

In all cases, the initial covariance matrix, $P_o$, had the following form

$$P_o = \begin{bmatrix} \sigma_r^2 & & & & & & & & & \\ & \sigma_r^2 & & & & & & & & \\ & & \sigma_r^2 & & & & & & & \\ & & & \sigma_v^2 & & & & & & \\ & & & & \sigma_v^2 & & & & & \\ & & & & & \sigma_v^2 & & & & \\ & & & & & & \sigma_\xi^2 & & & \\ & & & & & & & \sigma_\xi^2 & & \\ & & & & & & & & \sigma_\xi^2 & \\ & & & & & & & & & \sigma_T^2 \\ & & & & & & & & & & \sigma_T^2 \\ & & & & & & & & & & & \sigma_T^2 \end{bmatrix}$$

where $\sigma_r$ = 1000 meters, $\sigma_v$ = 1 meter/sec, $\sigma_T$ = .015 seconds, $\sigma_\xi$ = .0001 meters/sec$^2$. In general, the initial value of $\xi$ is taken to be zero unless otherwise stated.

**Results**

Not only were two types of gravity model errors studied, but the effects of observation noise, station location, and number of stations were investigated. These results are discussed in the following. The gravity model error due to a point mass will be referred to as Case I and the second type discussed in preceding sections will be referred to as Case II. Furthermore, Case I is only considered in the 50 cm range observations study.

1. 50-cm Range Observations

Both types of gravity model errors were used in the study with range observations in the noise level of 50 cm.

A. Case I

In the generation of the observations, a point mass of $3.64 \times 10^{-5}$ times the mass of the earth was placed at 41°N latitude and 108°W longitude. The standard deviation in the state noise was .005 and the initial value assumed for the time correlation coefficient, $T_i$, i = 1, 2, 3, was 200 seconds. Figure 2 shows the result of estimating the acceleration due to the model error, or

unmodeled acceleration. In this figure, the smooth line represents the true value and the jagged line represents the estimate. Figs. 2a, 2b, and 2c represent the acceleration components in a rectangular coordinate system. Note that the estimate follows the true acceleration component and that the estimate has a mean which is close to the true value. Figs. 2d and 2e, show the trace of the state error covariance matrix and the true error norm plotted as a function of time. In Fig. 2d, for example, the smooth line represents the trace of P associated with the position components and the jagged line represents the true error norm. It is important to note that the state error covariance matrix bounds the true error. In this case, 12 tracking stations were used, although not all stations can observe the satellite simultaneously as shown in Table II. Those not used were Merritt Island, Arecibo, and Bermuda. Since the true error is within one meter from 5 to 20 minues, the (O-C)'s would also be within one meter.

B. Case II

The gravity model error was simulated using $J_3$ through $J_6$ and the tesseral and sectorial harmonics through order four. The same stations used in Case I were also used in this case. Figure 3a, 3b, and 3c show the acceleration estimate and the true acceleration. The standard deviation in the state noise was 0.000025. Again, the smooth line is the true and the jagged is the estimate. Although the estimate of the acceleration is not as good as in Case I, the state estimate is quite good, that is, within one meter. It should be noted that the acceleration error is approximately 100 times smaller than in the preceding case. The acceleration error in Case II is on the order of 5-8 milligals, as can be seen in Fig. 3. The (O-C)'s are shown in Fig. 4. Note that most of the points are within the 50 cm noise level of observation.

As a point of comparison the same case was run using the batch processor. The (O-C)'s are shown in Fig. 5. Note the periodic-type behavior with amplitude considerably above the noise level of the observation.

Figure 6 shows the results obtained by replacing the Santa Barbara, Las Vegas, and Albuquerque stations by ones at Merritt Island, Arecibo, and Bermuda. The influence of additional east coast stations was not significant except toward the end of the pass. It can be seen in Fig. 2d that the error begins a significant increase at approximately 20 minutes. Table II shows that at about 20 minutes there are four stations taking data and beginning at 24 minutes, only one station taking data. The error growth appears to be an effect of the number of stations. This effect will be discussed in a later section.

2. 1-cm Range Observations

Repeating the preceding Case II with $\sigma$ = 50 cm replaced by $\sigma$ = 1 cm yielded the results shown in Fig. 7. The tracking stations not used were Merritt Island, Arecibo, and Bermuda. It is apparent that by improving the observation accuracy, the estimate of the unmodeled acceleration is improved also. The upward trend of the covariance trace in Fig. 7d is again an effect of a single station observing the satellite. Note, however, that the true error is not increasing. Figure 8 illustrates the (O-C)'s for two of the stations, Goldstone and Goddard. Note that most of the residuals are within the 1-cm observation noise. For comparison, the same case was run in a batch processor. The (O-C)'s resulting from this case are shown in Fig. 9.

Since it is evident that the accuracy with which the unmodeled acceleration can be estimated is dependent on the observation accuracy, Case I was not run with 1-cm observations since 50-cm observations gave good estimates. The 1-cm observations would simply reduce the scatter in the estimate.

3. 2mm/sec Range-Rate Observations

The Case II discussed in the preceding section (2) was repeated using range-rate observations of 2 mm/sec accuracy. The results are shown in Fig. 10. The accuracy with which the unmodeled acceleration can be estimated is comparable to the 1-cm range observations. The (O-C)'s behave as expected.

4. 25° Elevation Constraint

A case was run to examine the effect of a 25° elevation constraint on the 1-cm range observations. All observations yielding an elevation less than 25° were discarded. The observation interval used was .02 min = 1.2 sec. Again, Merritt Island, Arecibo, and Bermuda were not included. In this case, as can be seen in Table II, the first station which can see the satellite is San Francisco at approximately 3.6 minutes. Shortly thereafter, Santa Barbara acquires the satellite. Figure 11a shows that the acceleration estimate is poor until approximately 4 minutes at which time a third station acquires, namely, Goldstone. After this, the estimator yields good estimates. Thus, for the simulation, the horizon-to-horizon observations yield results representative of a more realistic case.

5. Effect of Number of Stations Observing

The preceding case indicated the effect of the number of tracking stations which can observe the satellite. Figure 12 shows the results of using only three stations, namely, San Francisco, Ft. Davis, and Goddard. The observation accuracy is 1-cm in range, and the observations are taken from horizon-to-horizon. Note the radical change in the Y-component (Fig. 12b) when the third station is included at approximately 8 minutes. Even after the San Francisco station is lost at 16 minutes, the estimate remains quite good until the Ft. Davis station loses acquisition. Thus, this result shows that three stations can yield a good result while two stations may yield comparable or reasonable results. The question of what a single station can do with this method was not thoroughly investigated.

## Summary

Based on the numerical results in the previous section, it can be concluded that the DMC method provides a significant improvement over the conventional batch method in estimating the state of a satellite in the presence of gravity model errors. The 50 cm range observations and 2 mm/sec range-rate observations are realistic while the 1 cm range observation will probably be available in the very near future. Using these observation accuracies, it was shown in the previous section that the accuracy with which the unmodeled acceleration can be estimated depends on the observation accuracy and the magnitude of the acceleration due to the model error. Even when good acceleration estimates are not obtained, the state estimate yields (O-C)'s within the observation noise. The number of tracking stations which can observe the satellite influences the acceleration estimate. The results indicate that two or three stations yield good estimates at the 1-cm range noise level.

Further work is in progress to determine whether the second-order Gauss-Markov process would yield a significant improvement over the first-order process used in this paper. Additional investigation of the number of tracking stations required as well as the effect of tracking station location errors is underway. Consideration is also being given in the use of the acceleration estimates to improve the mathematical model of the geopotential.

## References


Connolly, P. E., "Orbit Determination for Artificial Satellites in the Presence of Errors in the Geopotential Model," Applied Mechanics Research Laboratory Report 1048, The University of Texas at Austin, 1972.

Fehlberg, E., "Classical Fifth-, Sixth-, Seventh-, and Eighth-Order Runge-Kutta Formulas with Stepsize Control," NASA TR R-287, 1968.

Gaposchkin, E. M., and Lambeck, K., "1969 Smithsonian Standard Earth (II)," SAO Special Report 315, 1970.

Ingram, D. S., "Orbit Determination in the Presence of Unmodeled Accelerations," Applied Mechanics Research Laboratory Report 1022, 1971.

Ingram, D. S., and Tapley, B. D., "Estimation of Unmodeled Forces on a Lunar Satellite," AAAS/AIAA Astrodynamics Specialist Conference, Paper No. 71-371, 1971.

Jazwinski, A. H., Stochastic Processes and Filtering Theory, Academic Press, New York, 1969.

Jordan, S. K., "Self-Consistent Statistical Models for the Gravity Anomaly, Vertical Deflections, and Undulation of the Geoid," Journal of Geophysical Research 77, 3660-3670, 1972.

Kasper, J. F., Jr., "A Second-Order Markov Gravity Anomaly Model," Journal of Geophysical Research, 76, 7844-7849, 1971.

Kolenkiewicz, R., Private Communicaton, 1972.

Marsh, J. G. and Douglas, B. C., "Tests and Comparisons of Gravity Models," Celestial Mechanics, IV, 309-325, 1971.

Melbourne, W. G., et. al., "Constants and Related Information for Astrodynamic Calculations, 1968," JPL TR 32-1306, 1968.

Muller, P. M. and Sjogren, W. L., "Lunar Gravimetry and Mascons," Applied Mechanics Reviews, 955-959, 1971.

Shaw, L., Paul, I., and Henrikson, P., "Statistical Models for the Vertical Deflection from Gravity-Anomaly Models," Journal of Geophysical Research, 74, 4259-4265, 1969.

Sjogren, W. L. , and Muller, P. M., "Lunar Surface Mass Distribution From Dynamical Point Mass Solutions," The Moon II, 338-353, 1971.

Smith, D. E., Kolenkiewicz, R., and Dunn, P. J., "Geodetic Studies by Laser Ranging to Satellites," Goddard Space Flight Center Report X-553-71-361, 1971.

Tapley, B. D., and Ingram, D. S., "Orbit Determination in the Presence of Unmodeled Accelerations," Proc. of the Second Symposium on Nonlinear Estimation Theory, San Diego, California, 1971.

Tapley, B. D., and Schutz, B. E., "Estimation of Unmodeled Forces on a Lunar Satellite," Paper to be presented at 23rd Congress of the IAF, Vienna, Austria, 1972.

Yionoulis, S. M., Heuring, F. T., and Guier, W. H., "A Geopotential Model (APL 5.0-1967) Determined from Satellite Doppler Data at Seven Inclinations," Journal of Geophysical Research 77, 3671-3677, 1972.

## Table I.

Initial Conditions (Meters and Meters/Sec.)

| | TRUE | NOMINAL | DIFFERENCE (TRUE-NOMINAL) |
|---|---|---|---|
| X | -5385692.8 | -5385610.2 | -82.6 |
| Y | -3576430.5 | -3576222.4 | -208.1 |
| Z | 3549660.3 | 3549464.8 | 195.5 |
| $\dot{X}$ | 5014.492 | 5015.173 | -.680 |
| $\dot{Y}$ | -4153.014 | -4153.526 | .512 |
| $\dot{Z}$ | 3411.811 | 3411.019 | .792 |

Horizon-to-Horizon Station Coverage

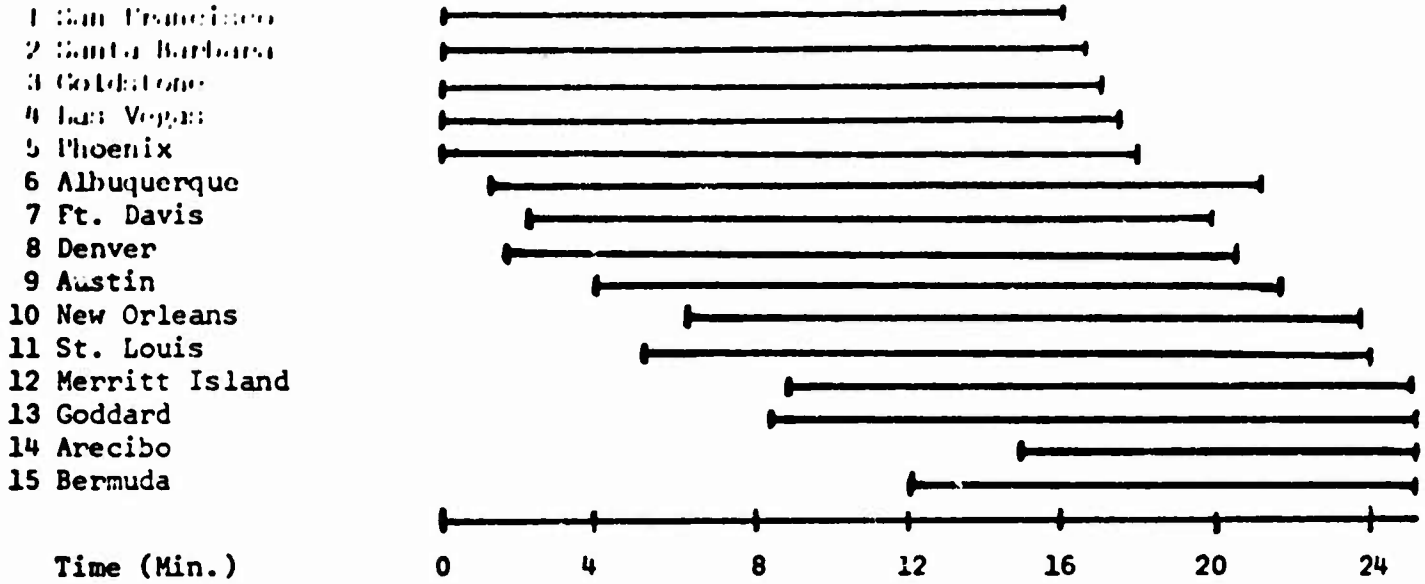


25° Elevation Constraint Station Coverage

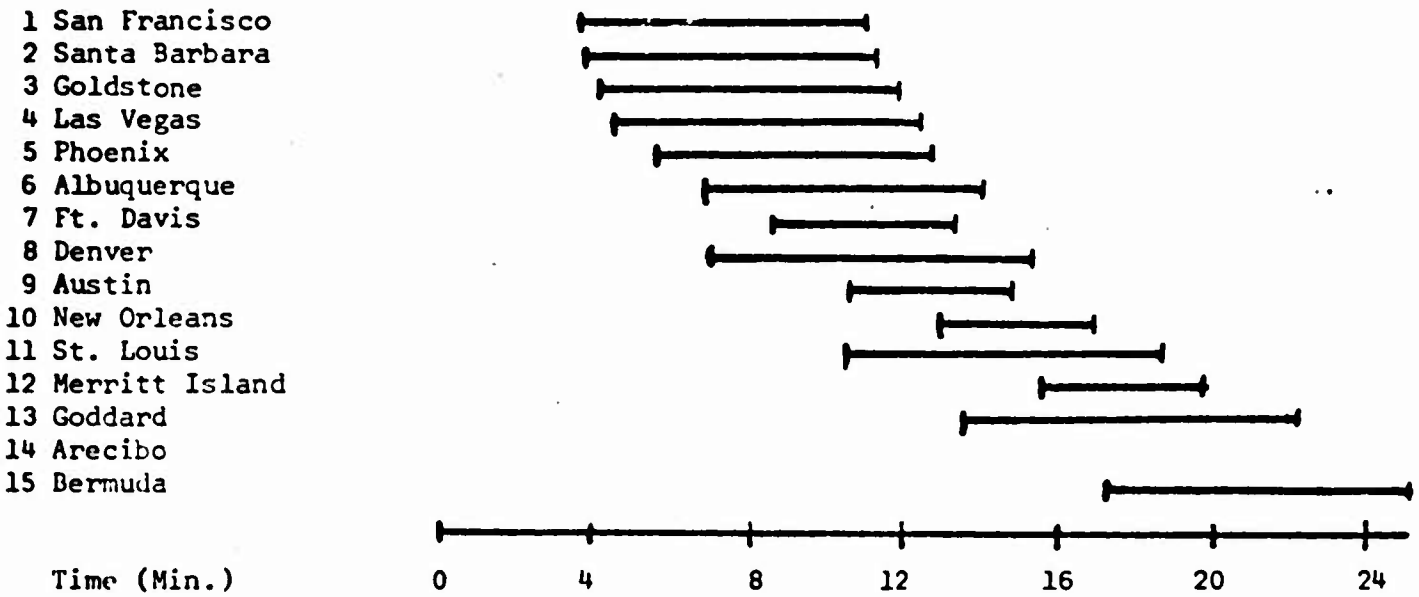


Table II

Simulation Tracking Station Locations and Coverage

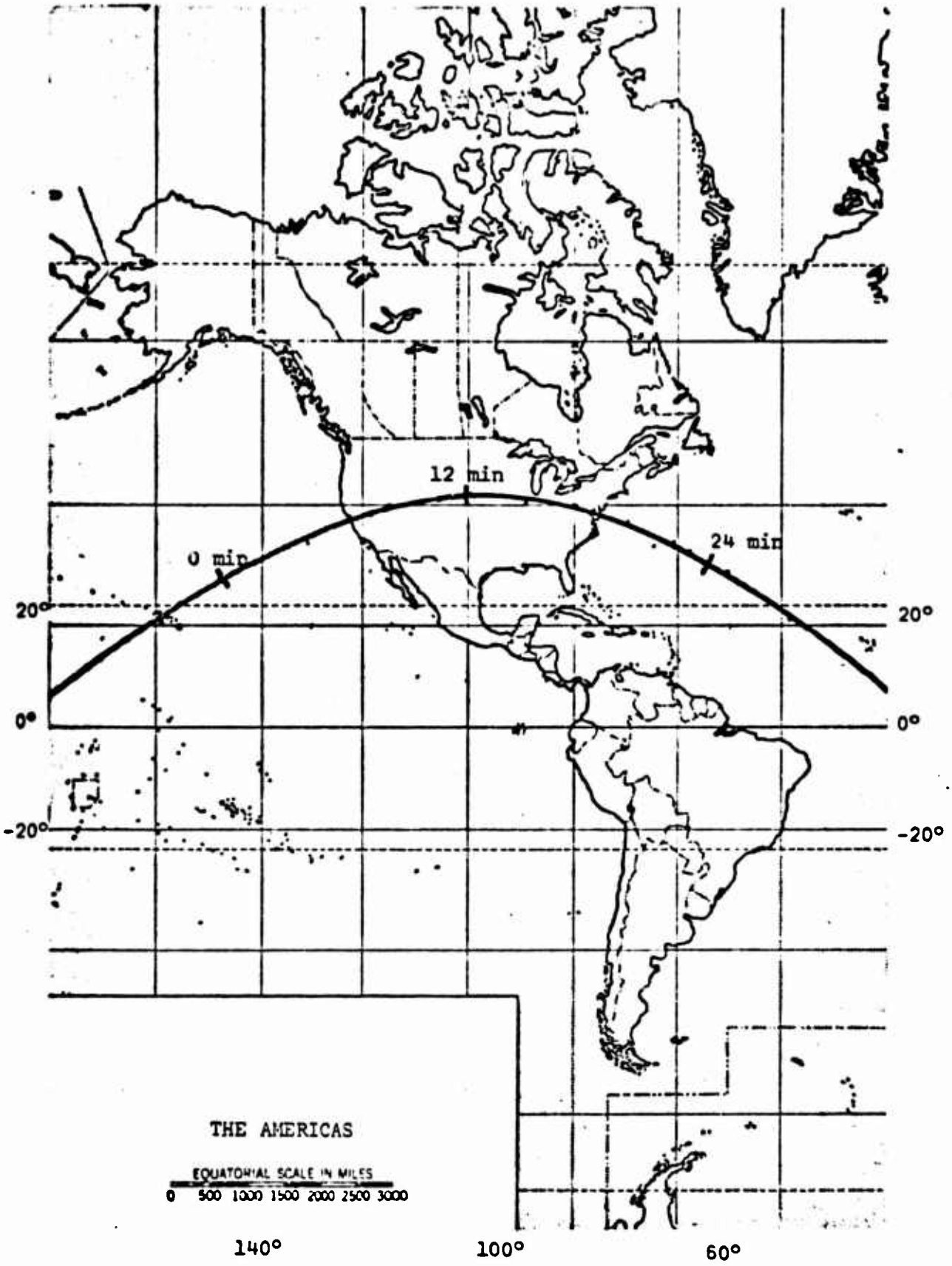


Figure 1. Ground Track of Satellite

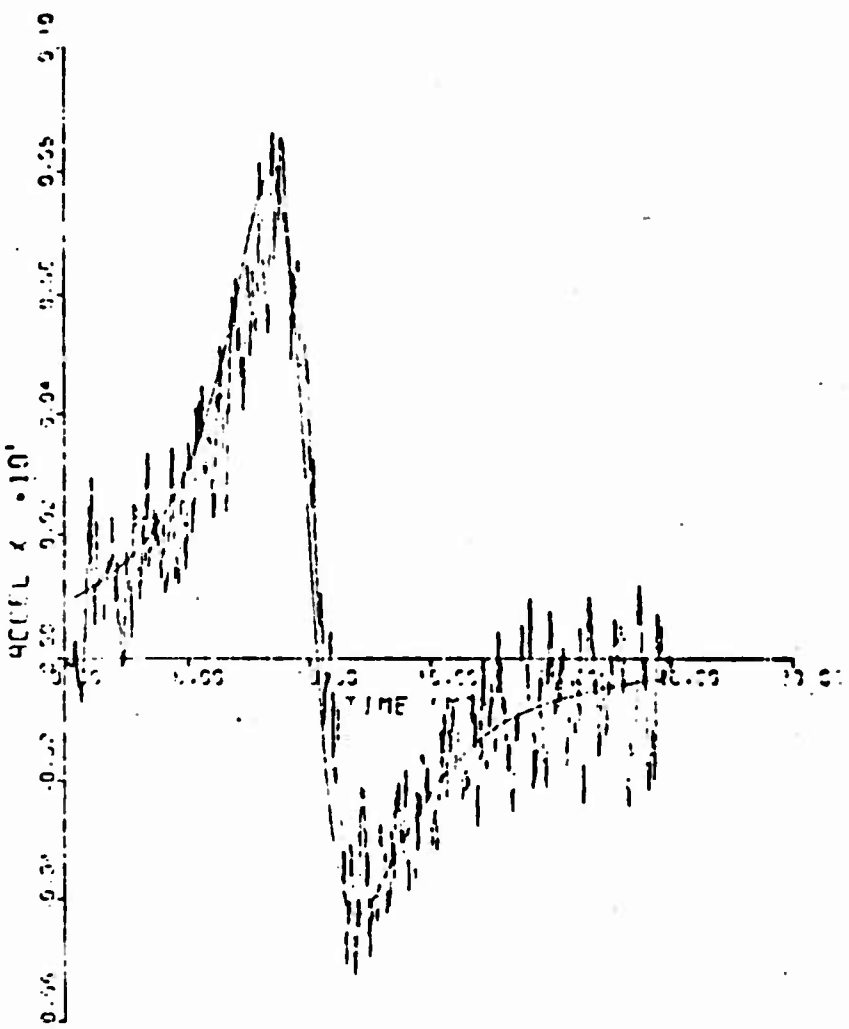

a. X Acceleration (meters/sec$^2$)

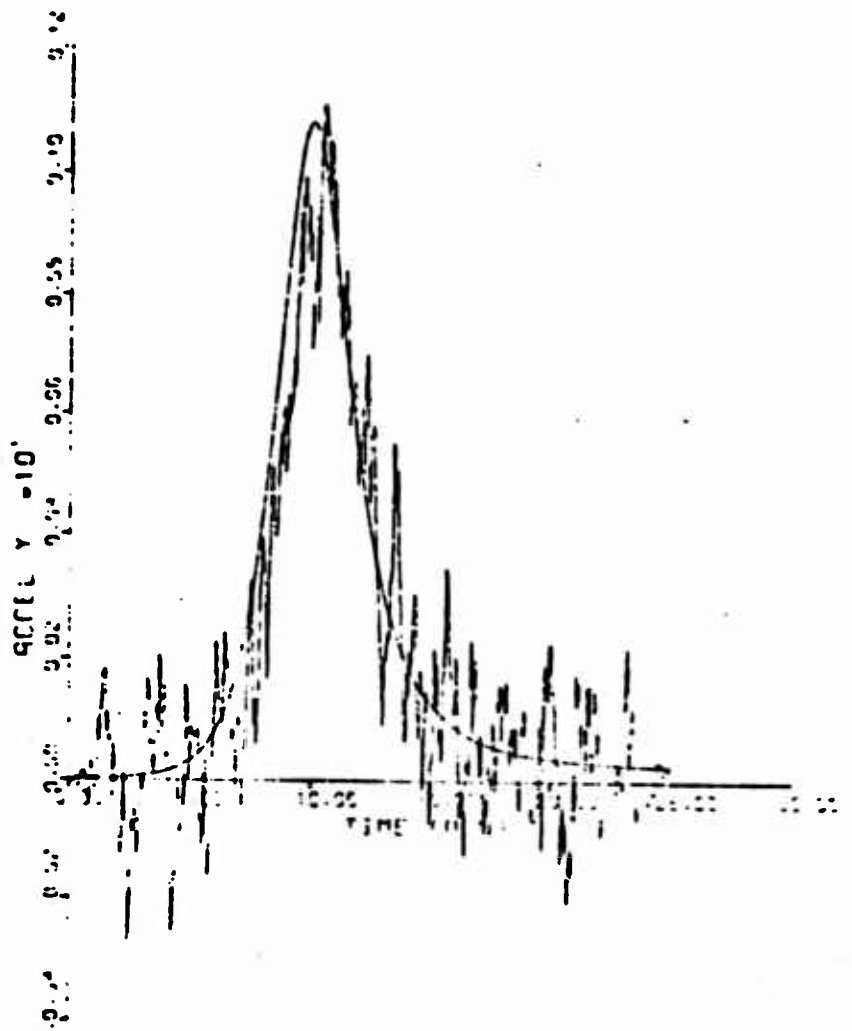

b. Y Acceleration (meters/sec$^2$)

Figure 2. Case I Model Error

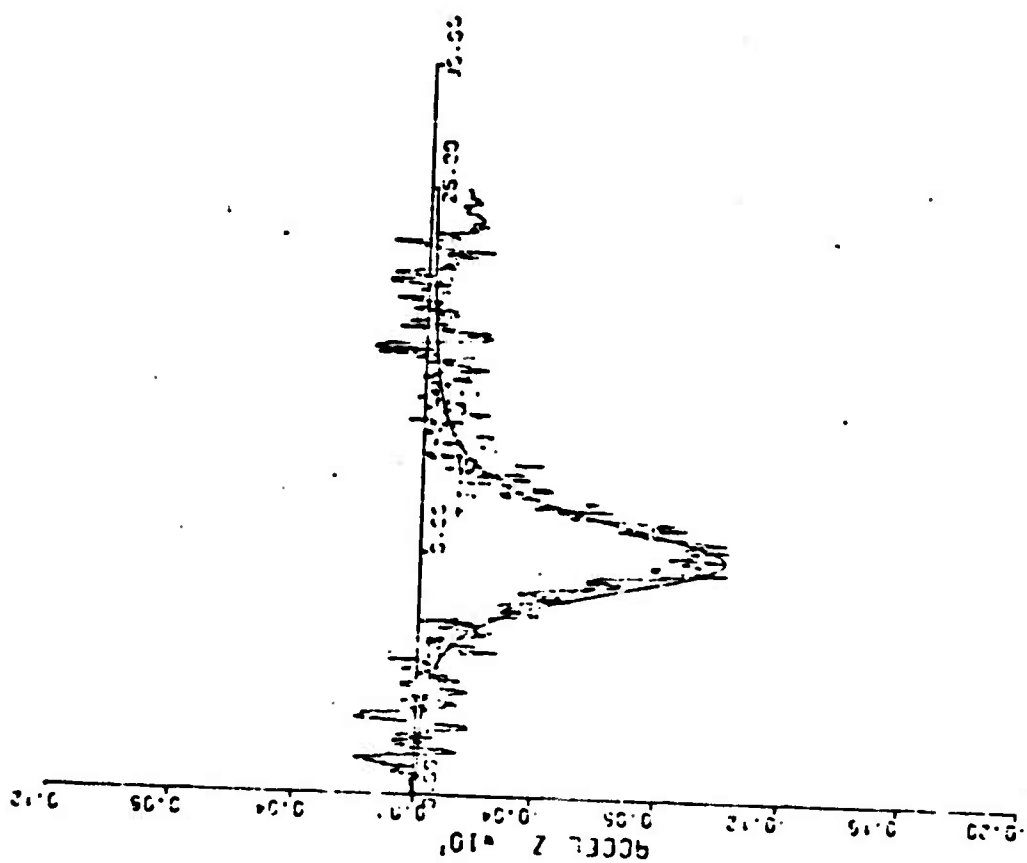

c. Z Acceleration (meters/Sec$^2$)

Figure 2. (Cont.)

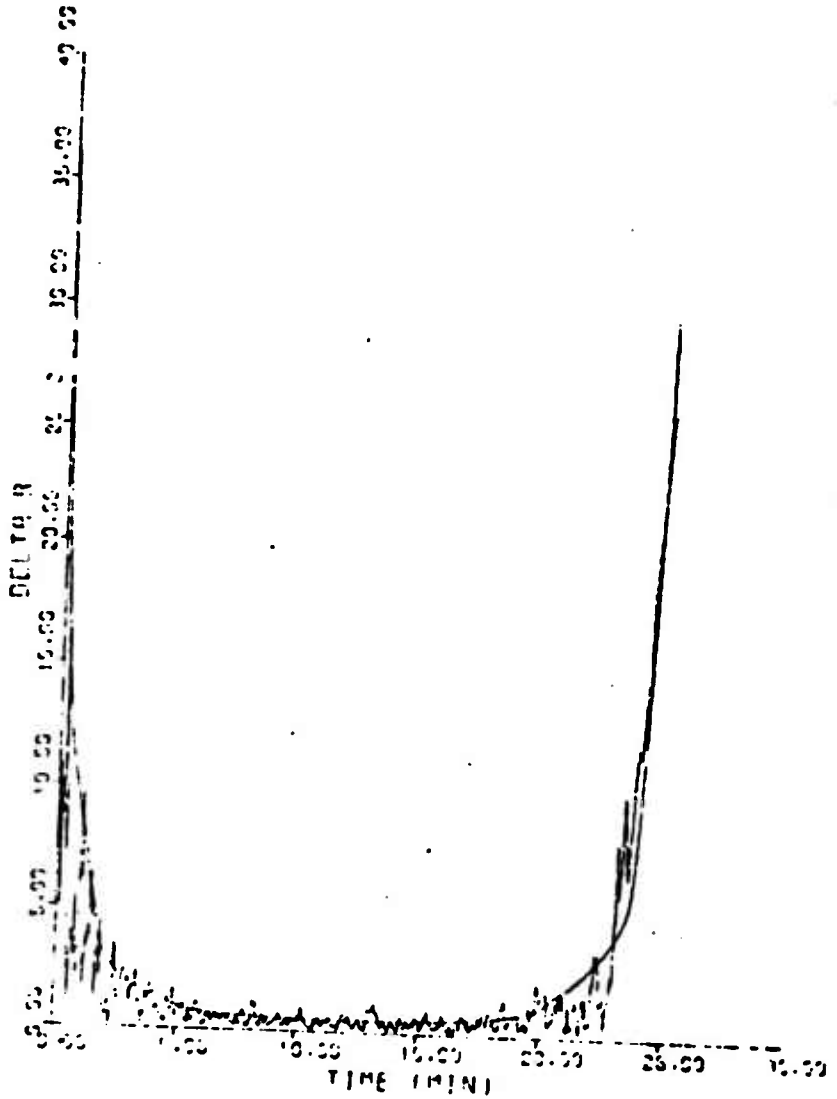


d. Position Error Norm (meters)

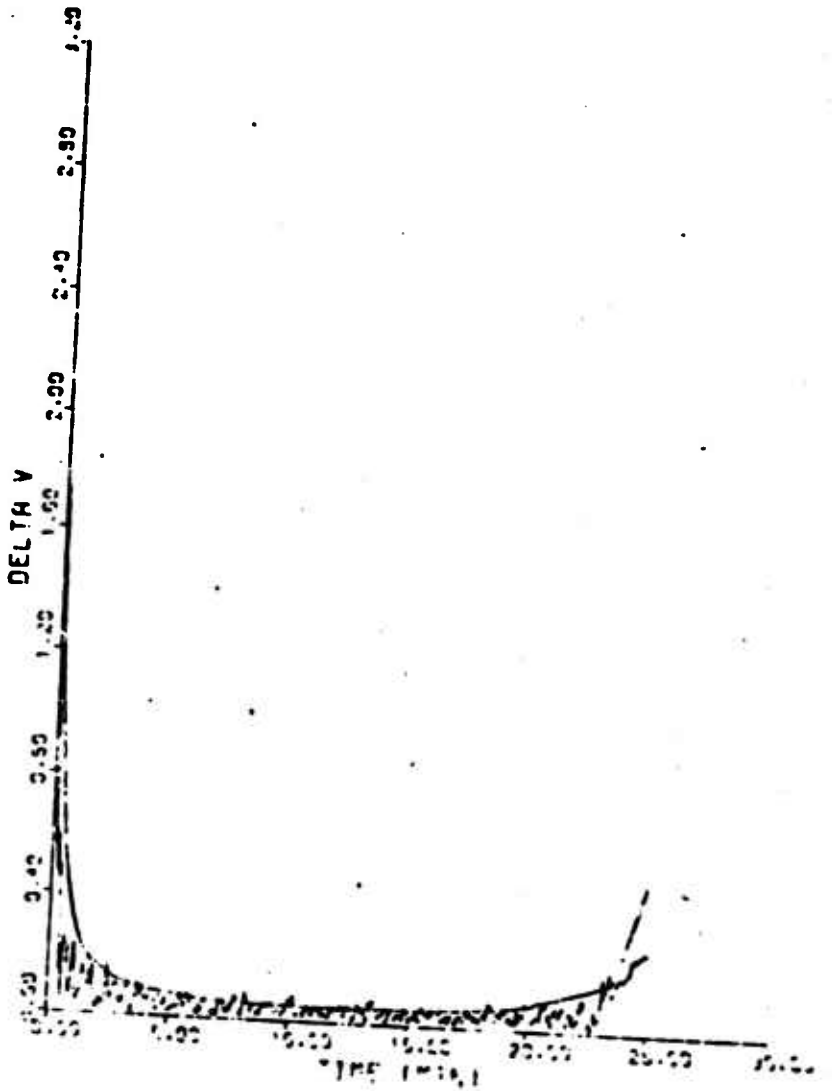


e. Velocity Error Norm (meters/sec)

Figure 2. (Cont.)

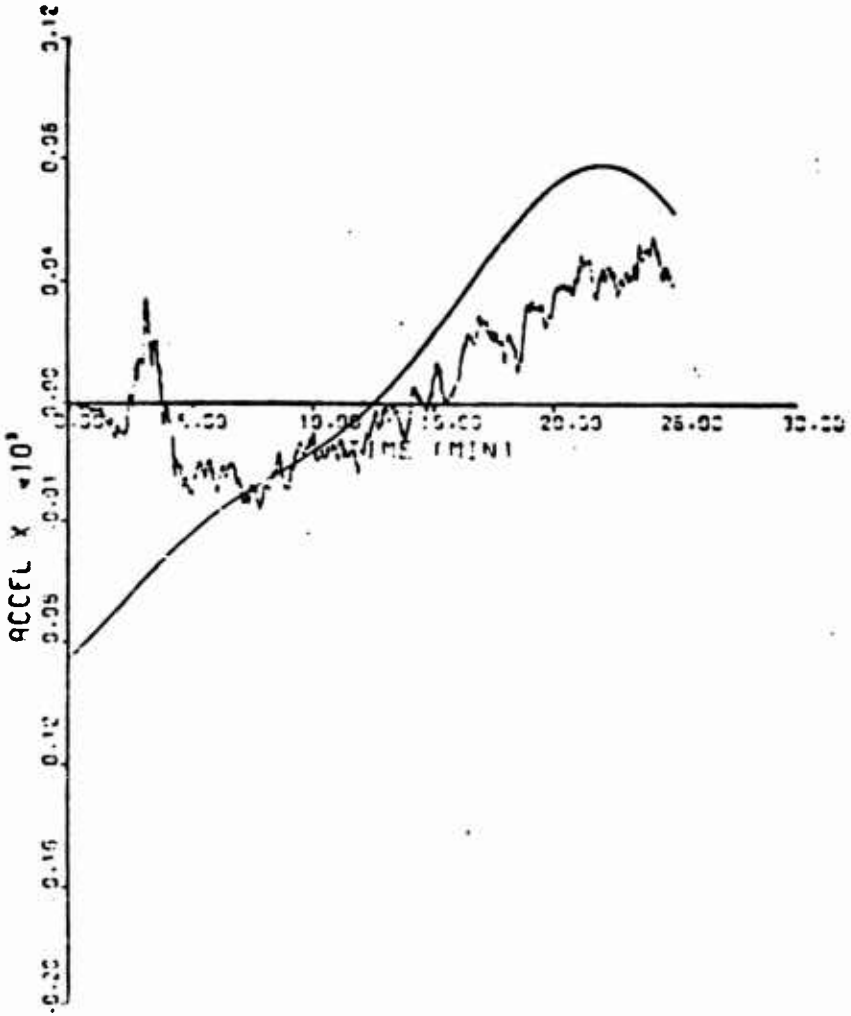


a. X Acceleration (meters/sec$^2$)

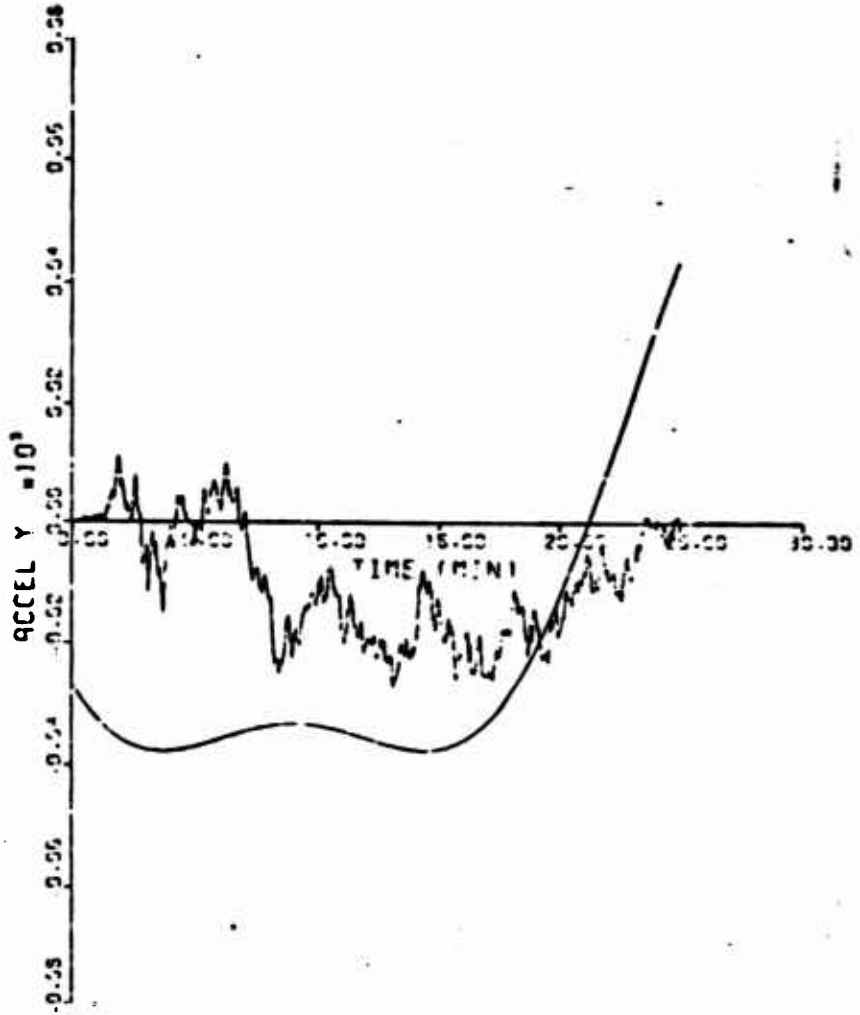


b. Y Acceleration (meters/sec$^2$)

Figure 3. Case II Model Error, $\sigma_\rho$ = 50 cm

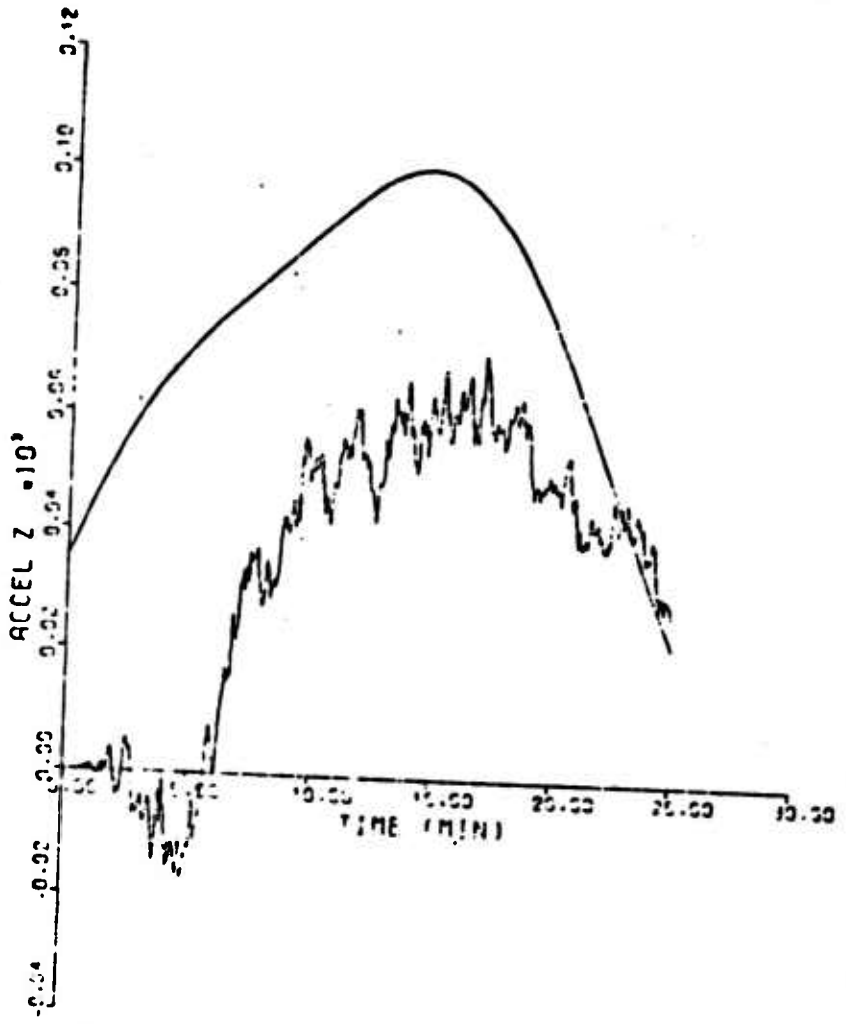


c. Z Acceleration (meters/sec$^2$)

Figure 3 (Cont.)

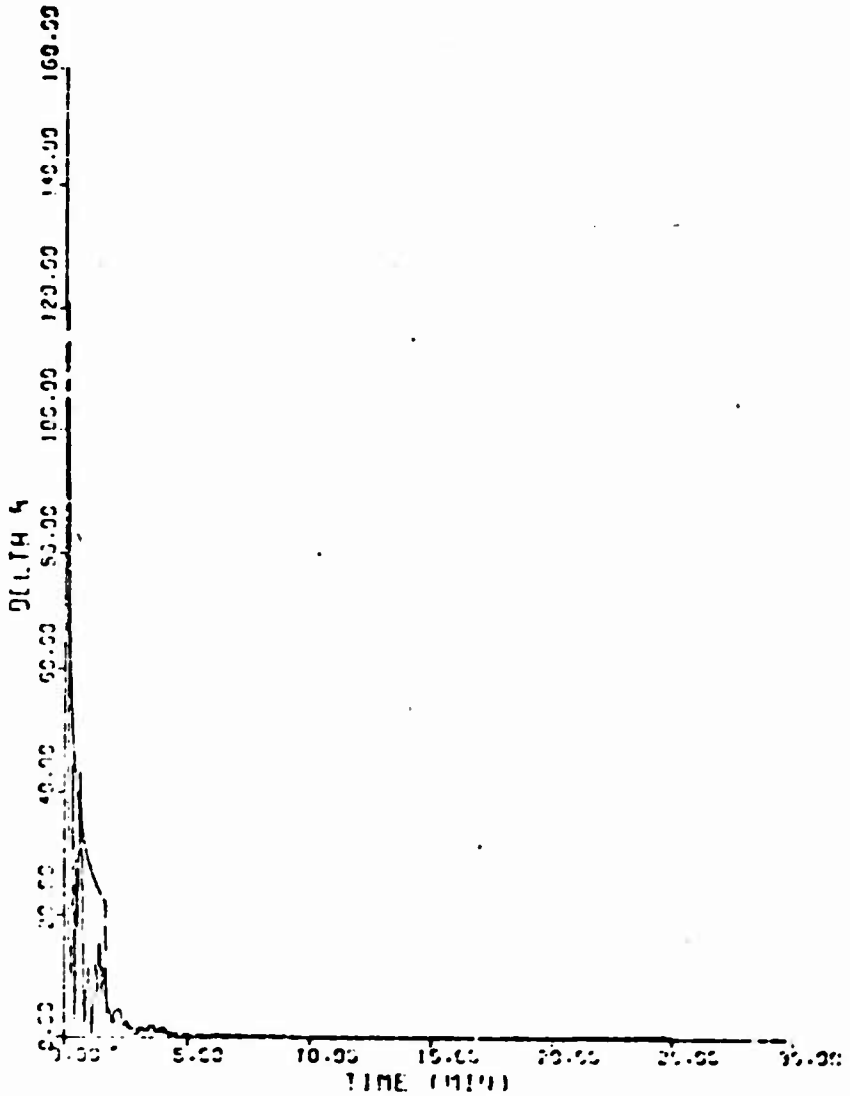


d. Position Error Norm (meters)

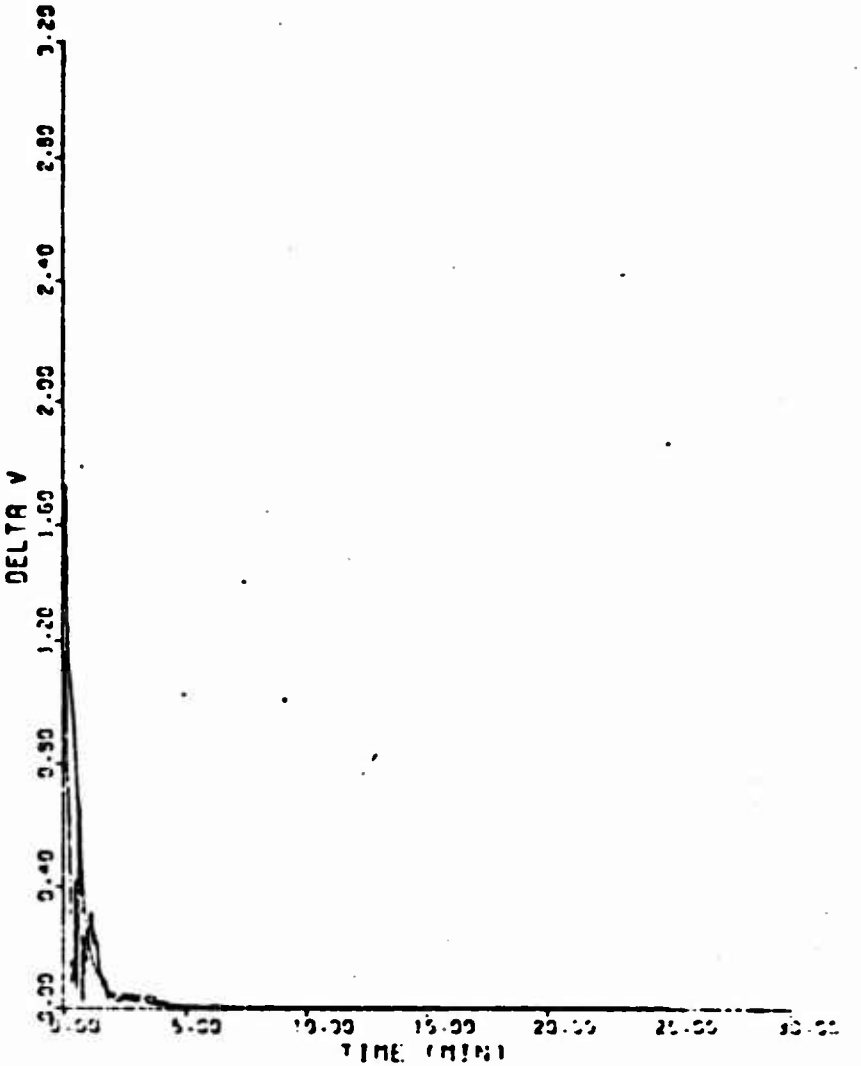


e. Velocity Error Norm (meters/sec.)

Figure 3 (Cont.)

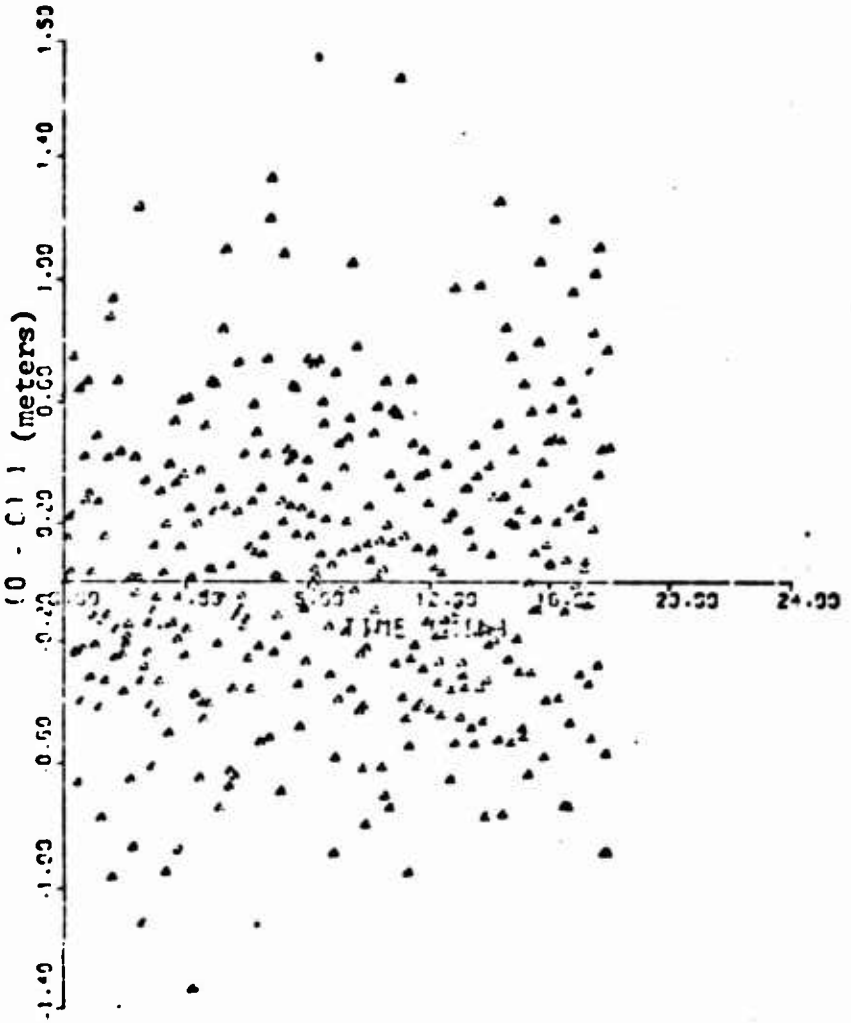

a. Goldstone

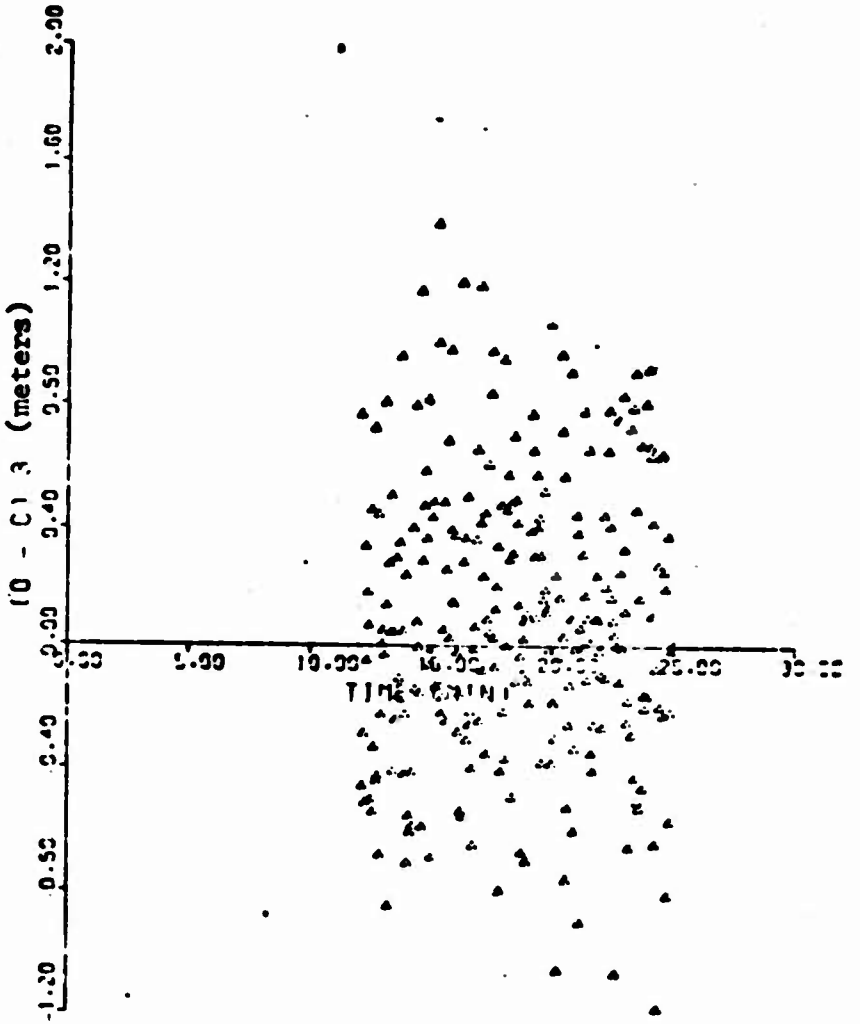

b. Goddard

Figure 4. (O-C) For the DMC Method

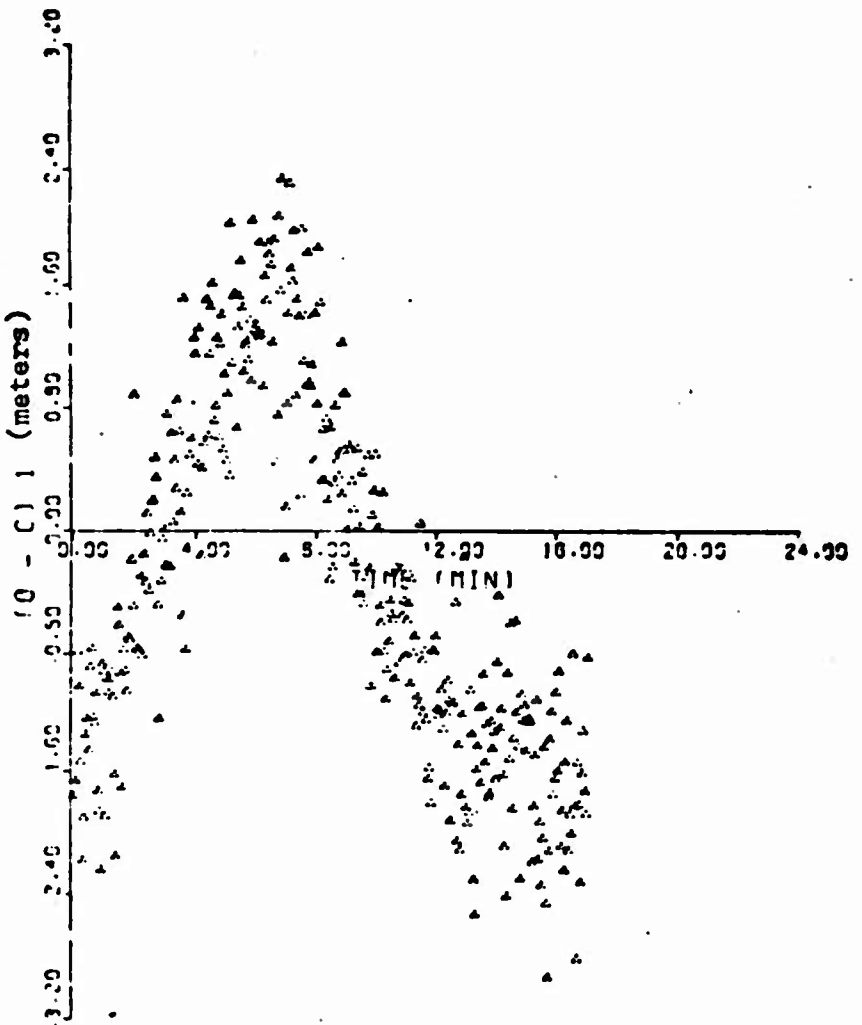


a. Goldstone

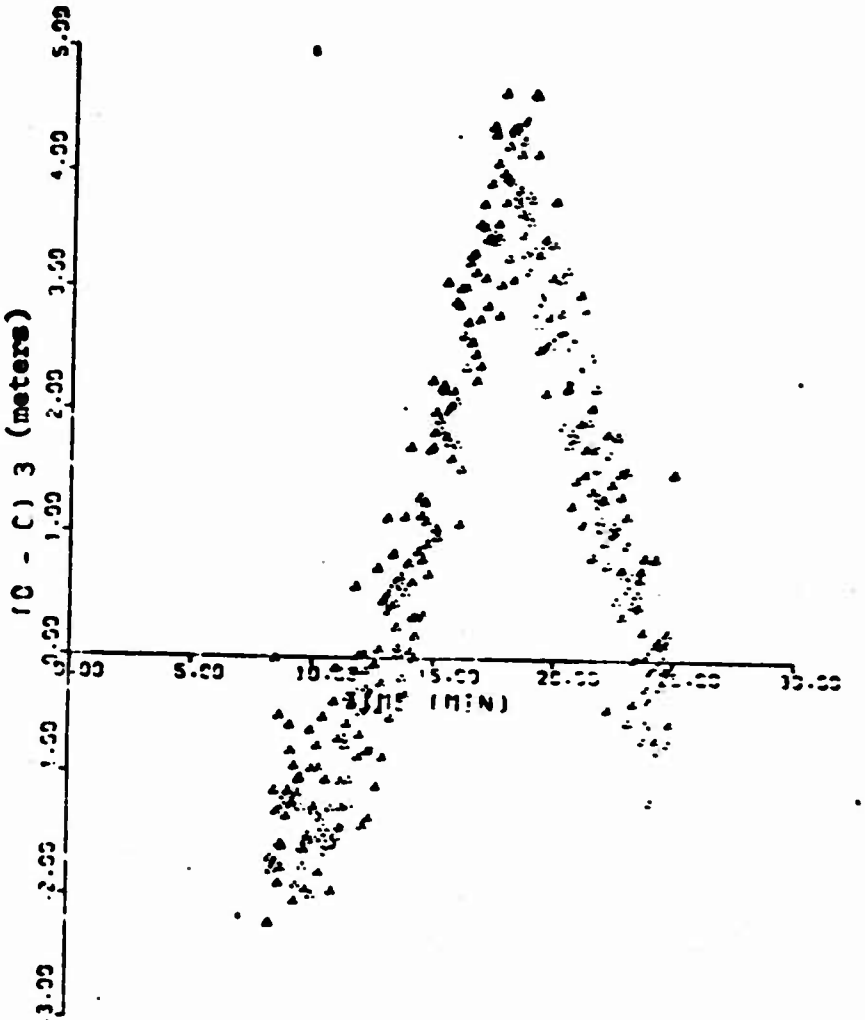


b. Goddard

Figure 5. (O-C) For The Batch Processor

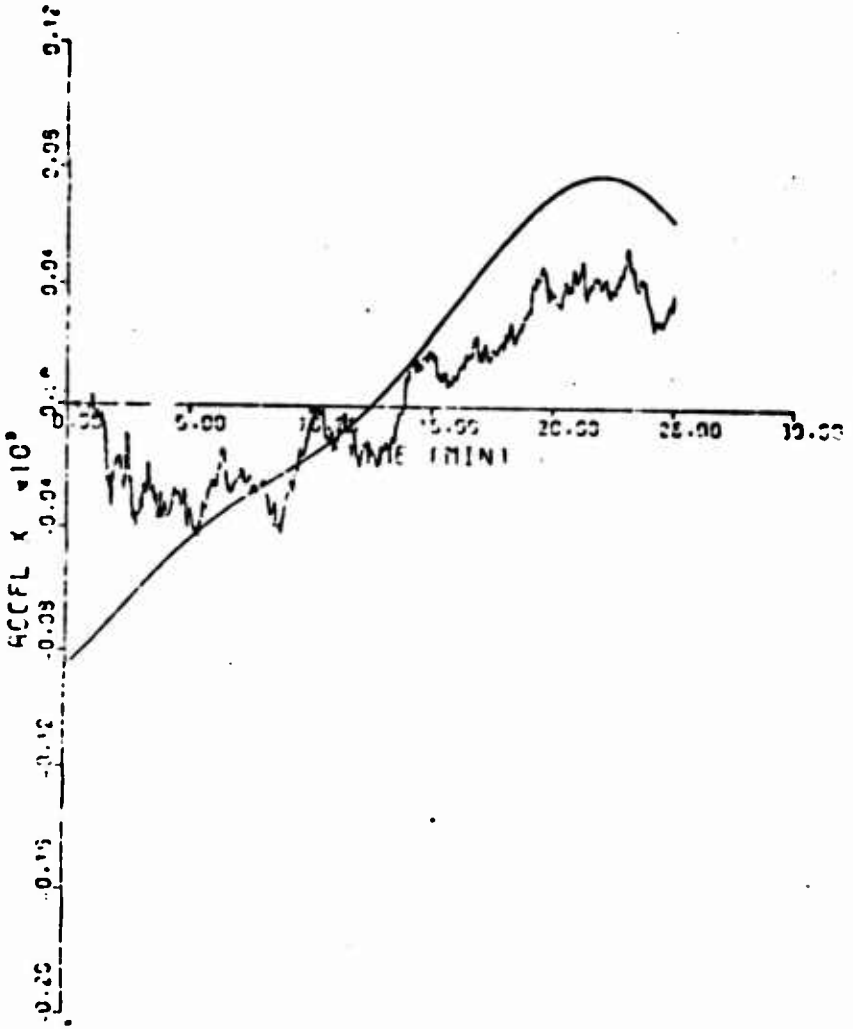


a. X Acceleration (meters/sec$^2$)

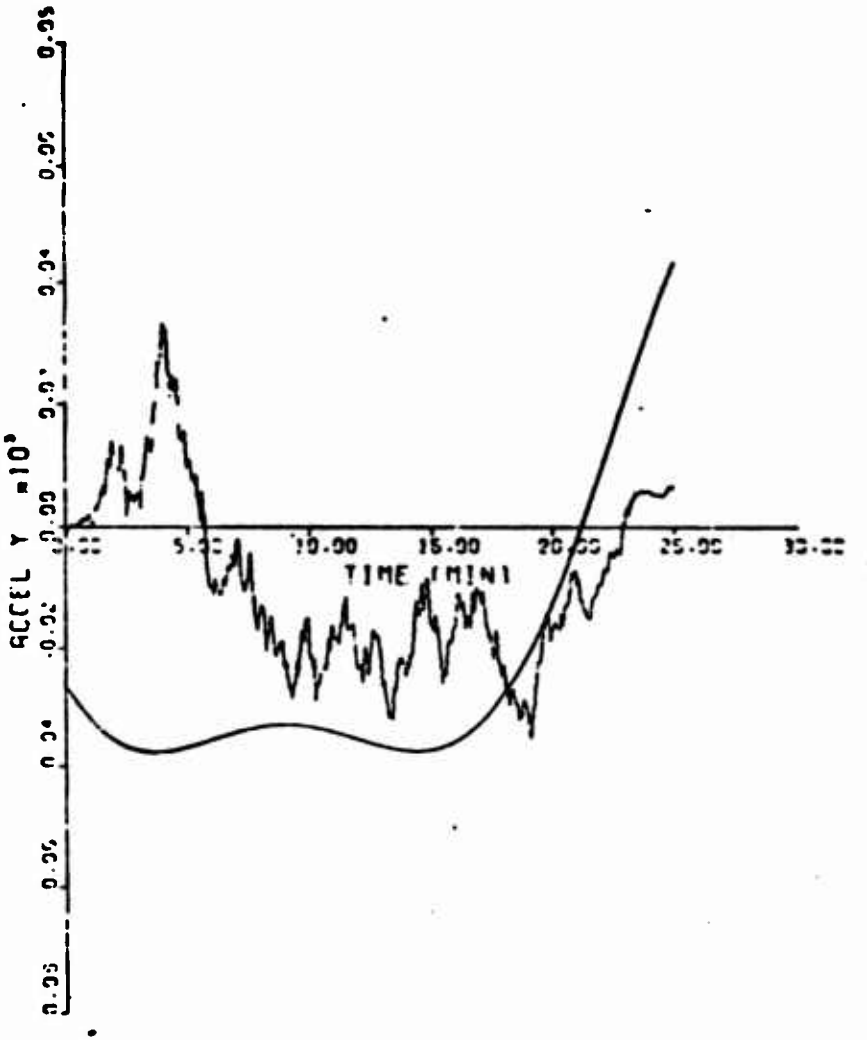


b. Y Acceleration (meters/sec$^2$)

Figure 6. Case II Model Error (Different Stations than Fig. 3)

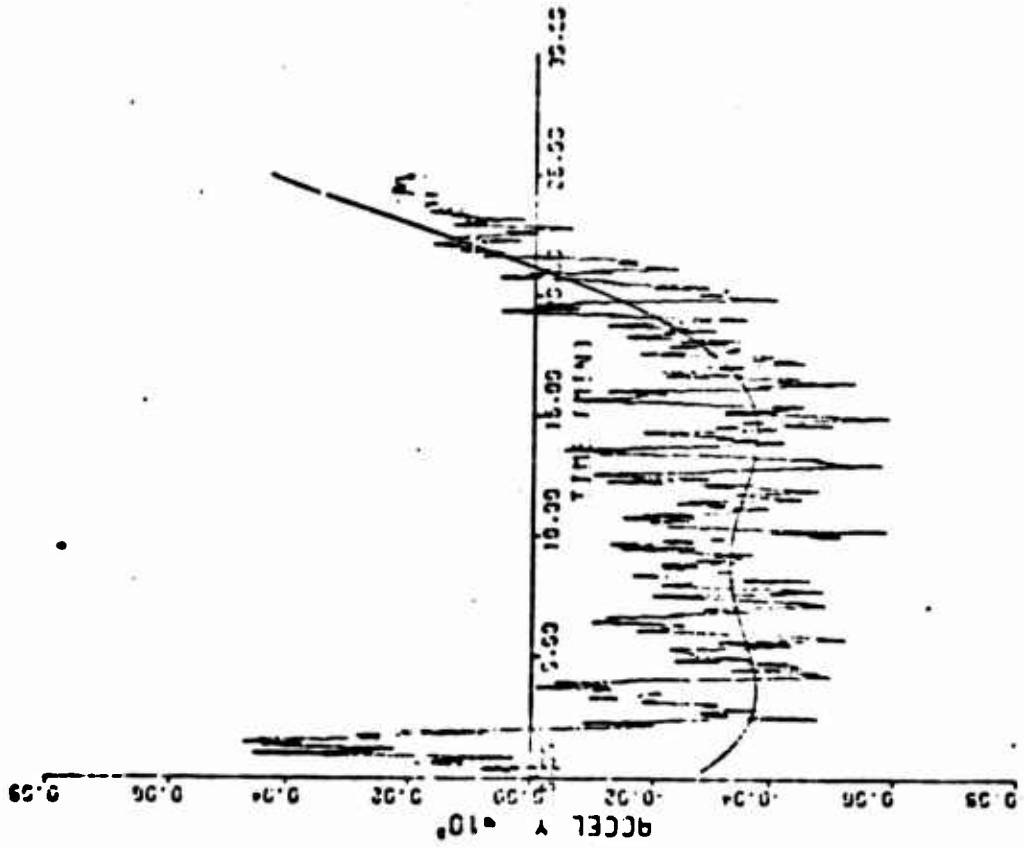

b. Y Acceleration (meters/sec$^2$)

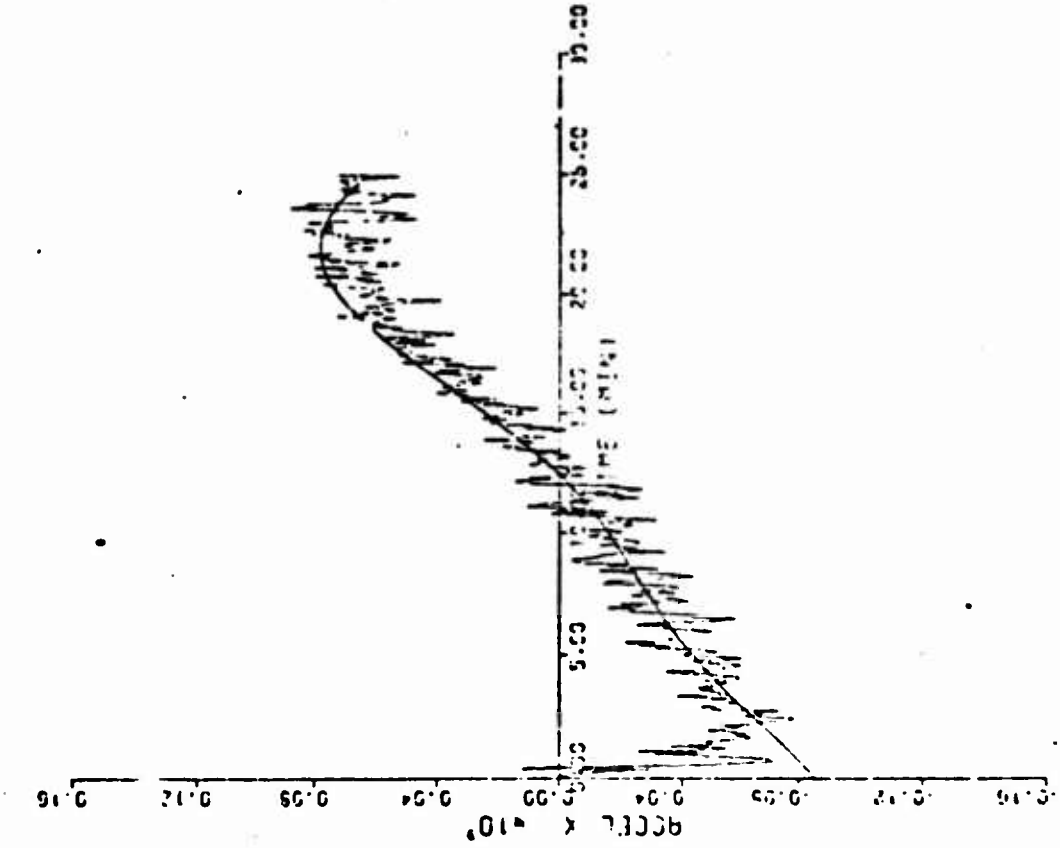

a. X Acceleration (meters/sec$^2$)

Figure 7. Case II Model Error, $\sigma_\rho$ = 1 cm

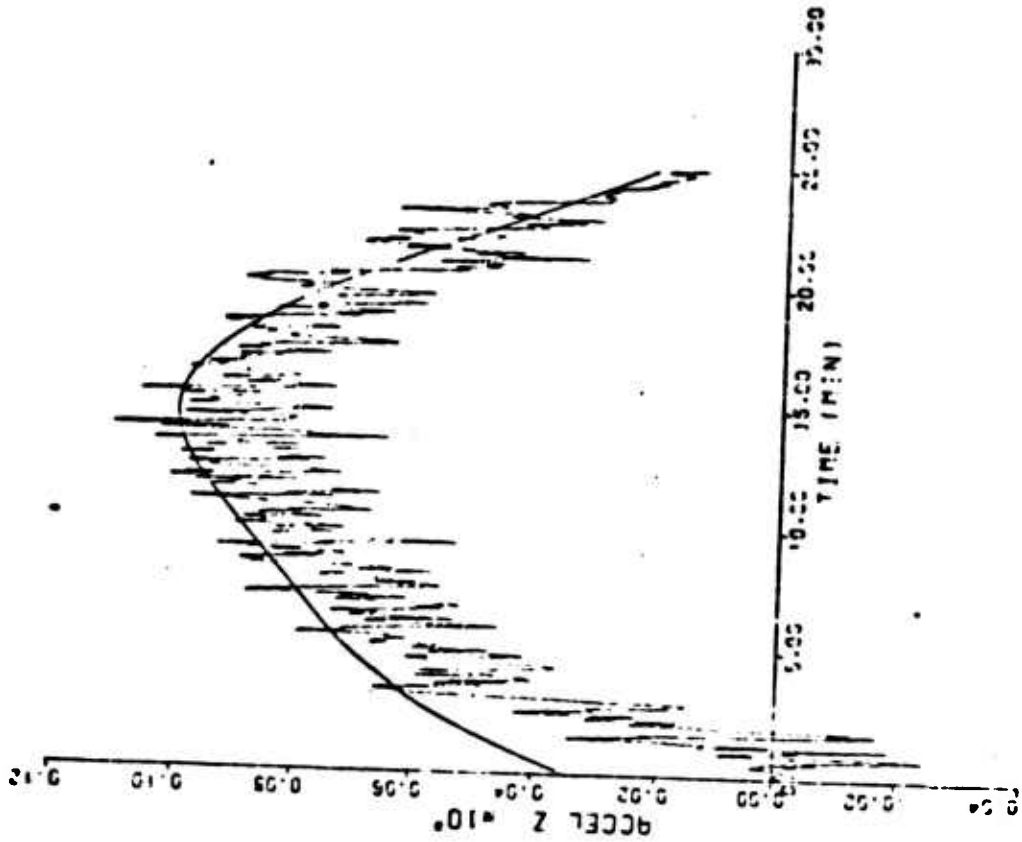


c. Z Acceleration (meters/sec$^2$)

Figure 7 (Cont.)

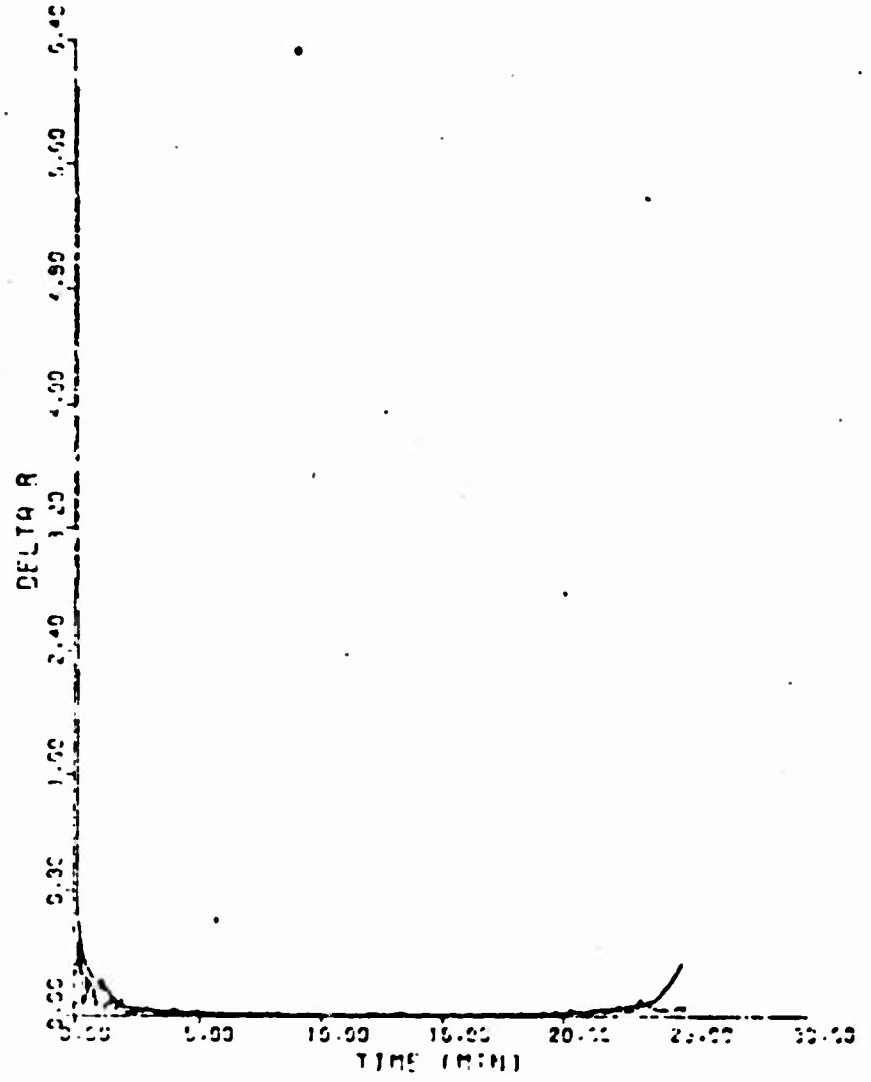


d. Position Error Norm (meters)

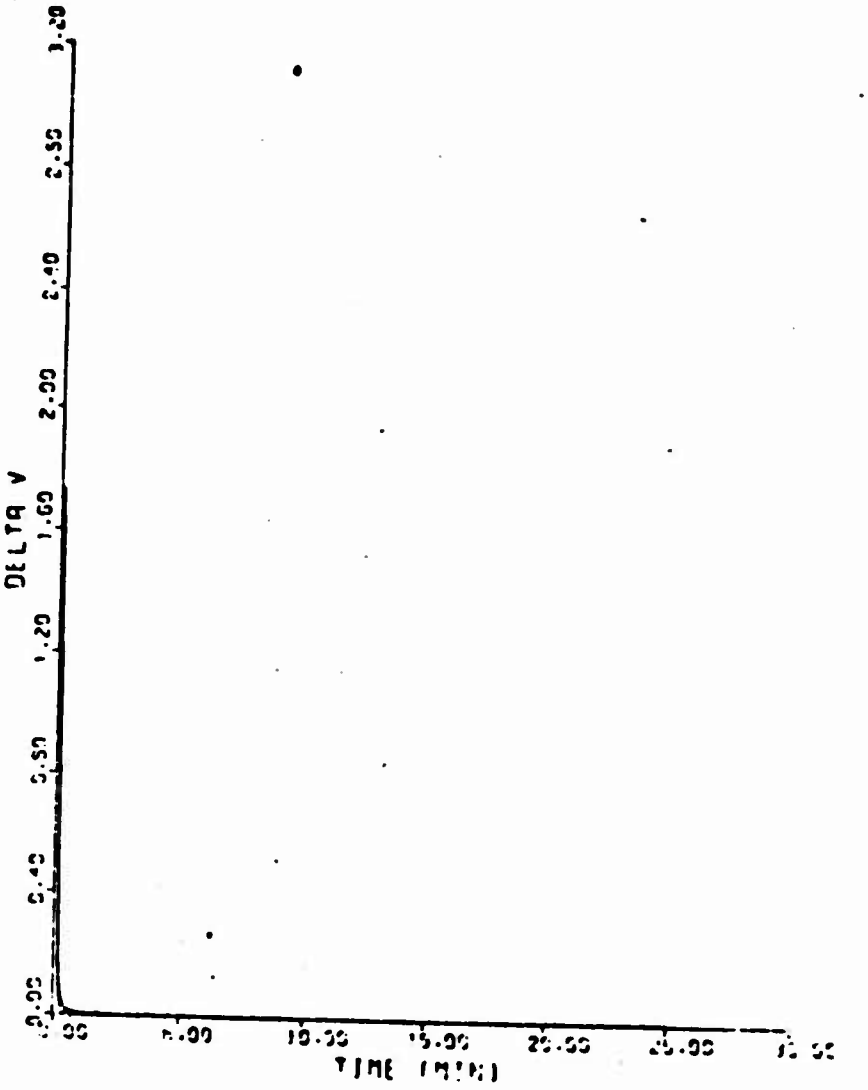


e. Velocity Error Norm (meters/sec)

Figure 7 (Cont.)

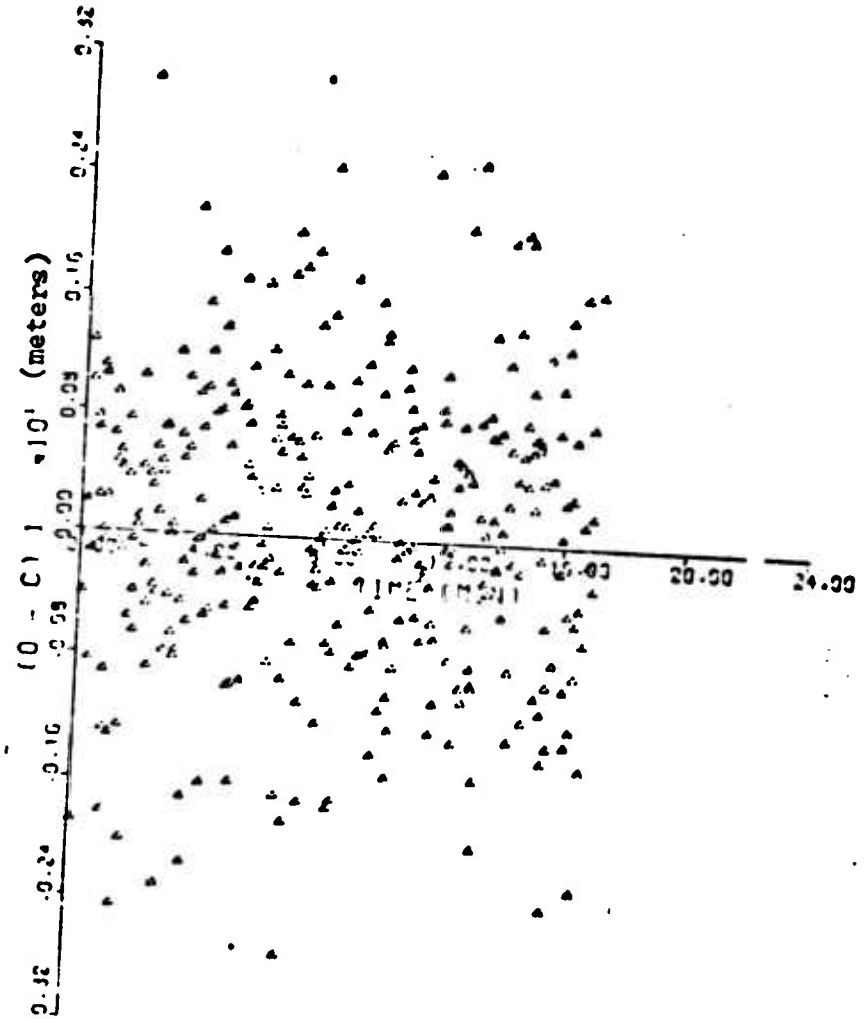


a. Goldstone

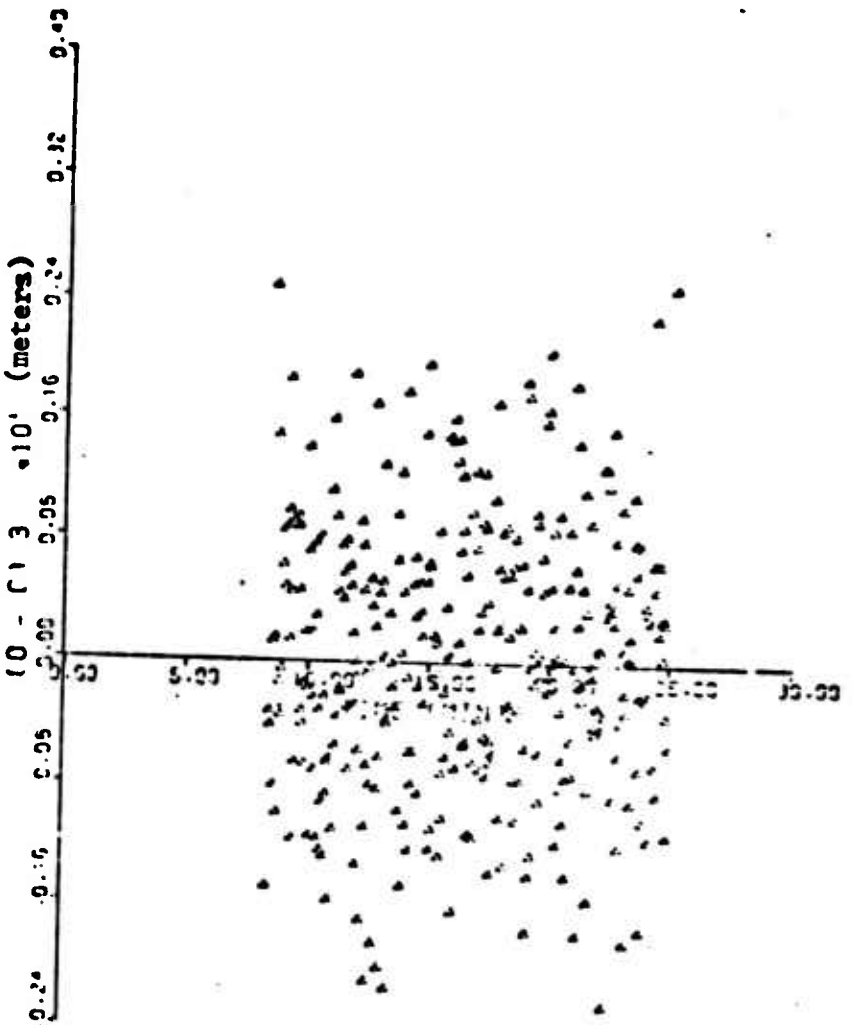


b. Goddard

Figure 8. (O-C) For the DMC Method

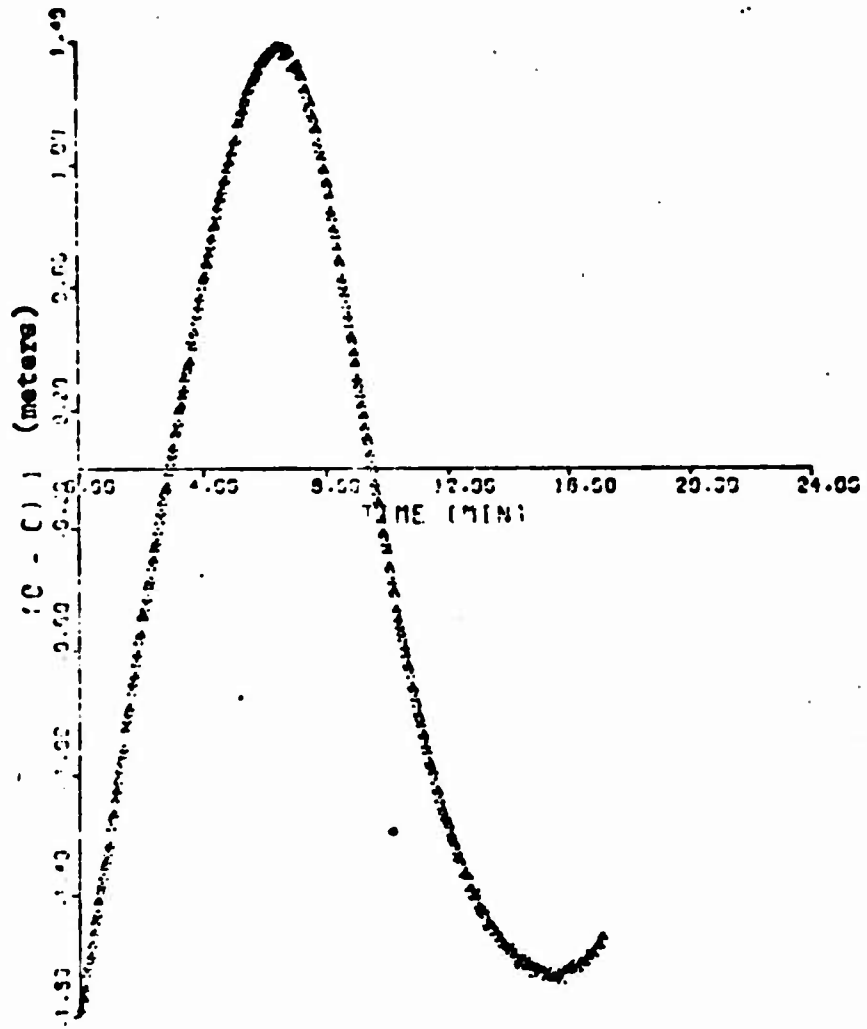


a. Goldstone

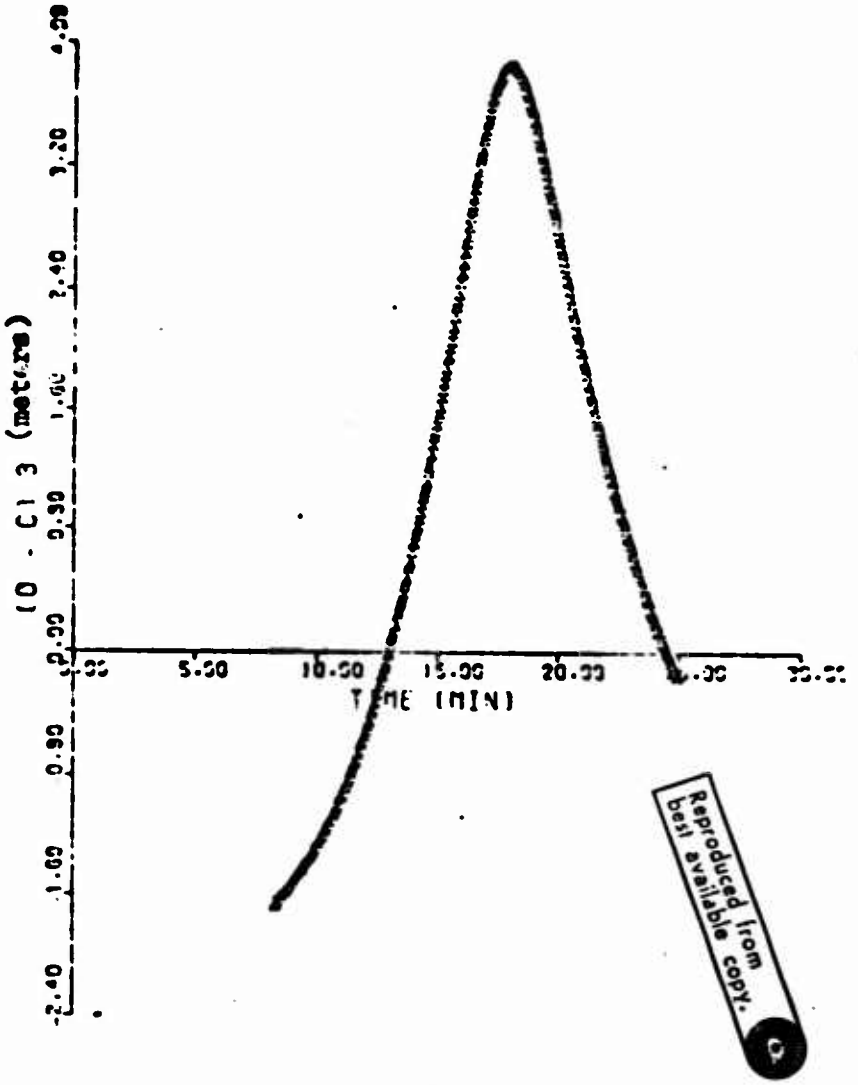


b. Goddard



Figure 9. (O-C) For the Batch Processor

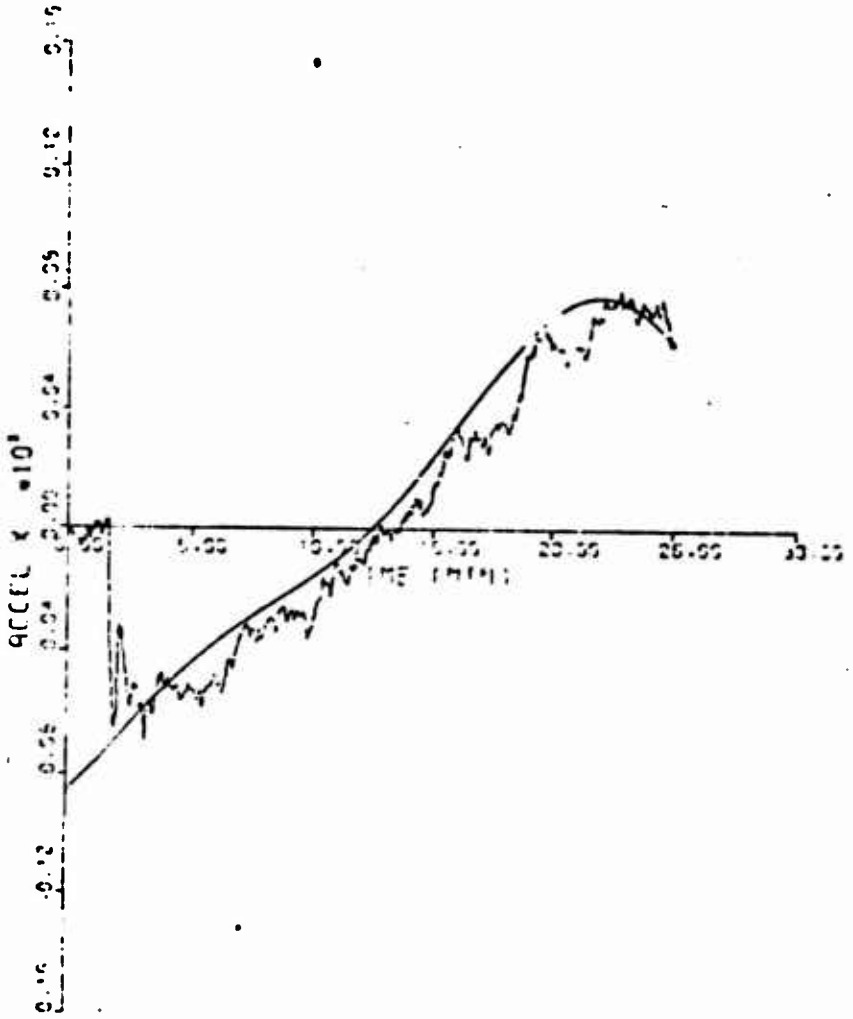

a. X Acceleration (meters/sec$^2$)

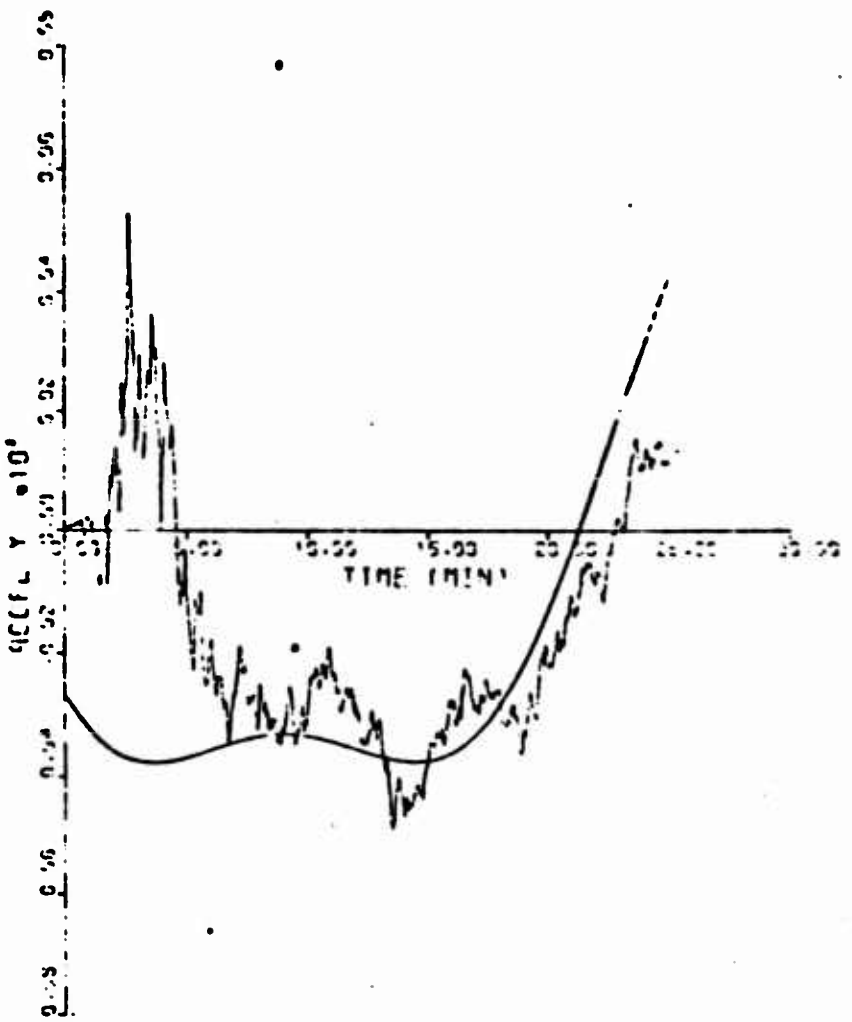


b. Y Acceleration (meters/sec$^2$)

Figure 10. Case II Model Error, $\sigma_{\dot{\rho}}$ = 2 mm/sec

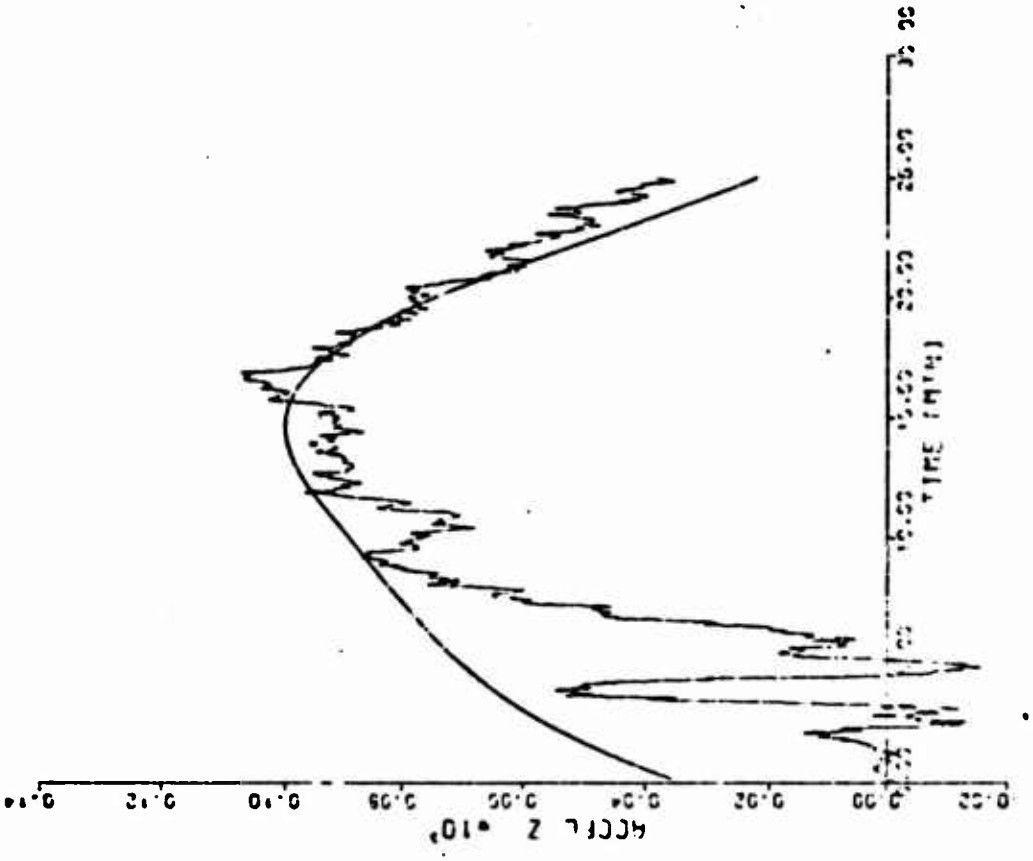

c. Z Acceleration (meters/sec$^2$)

Figure 10 (Cont.)

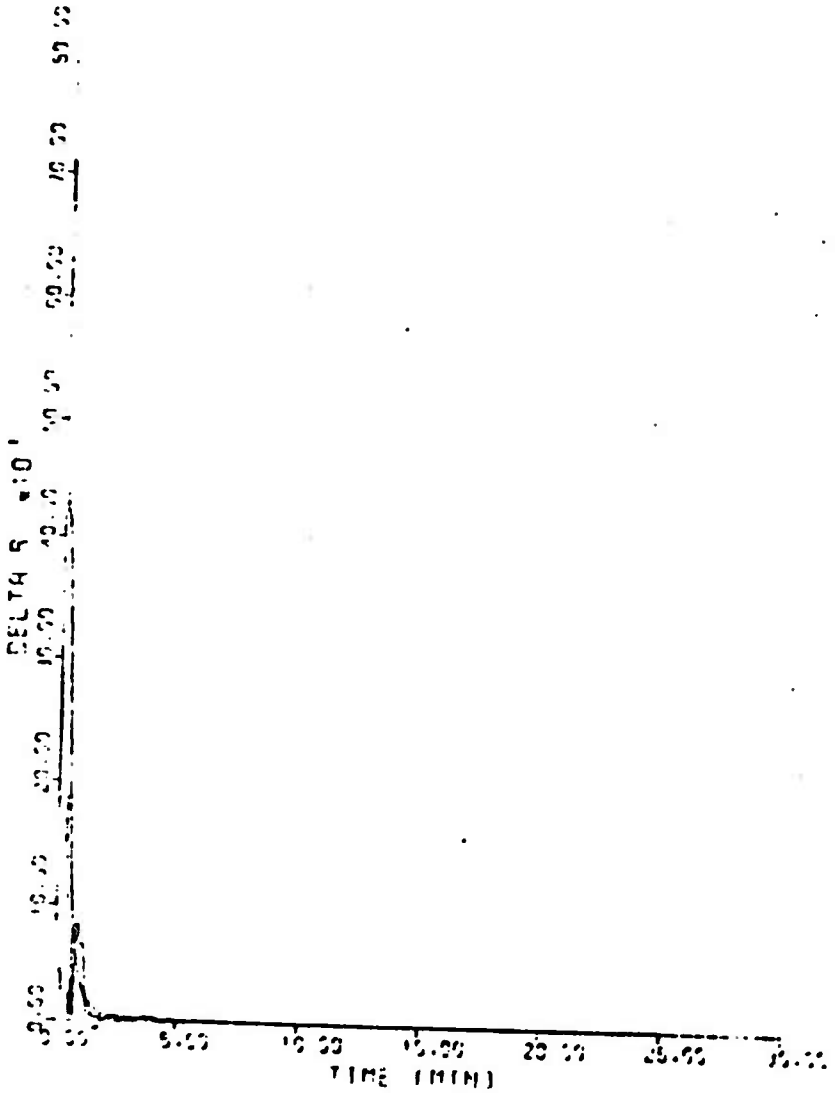


d. Position Error Norm (meters)

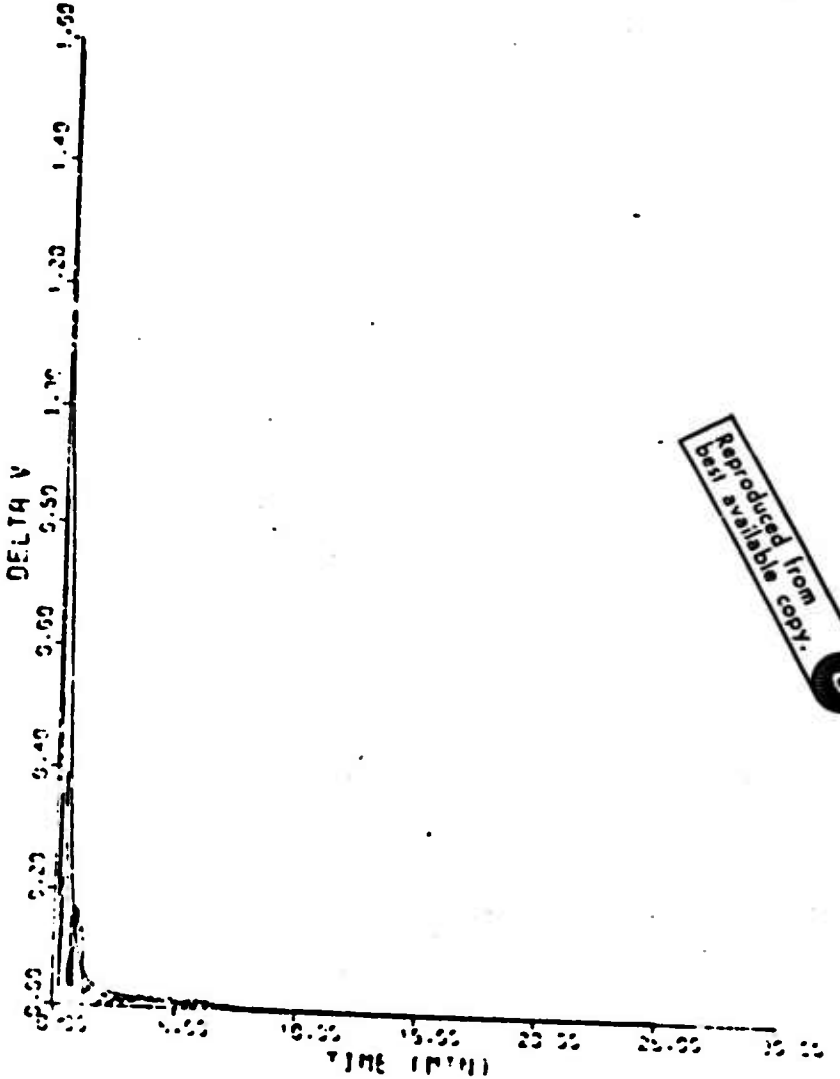


e. Velocity Error Norm (meters/sec)



Figure 10 (Cont.)

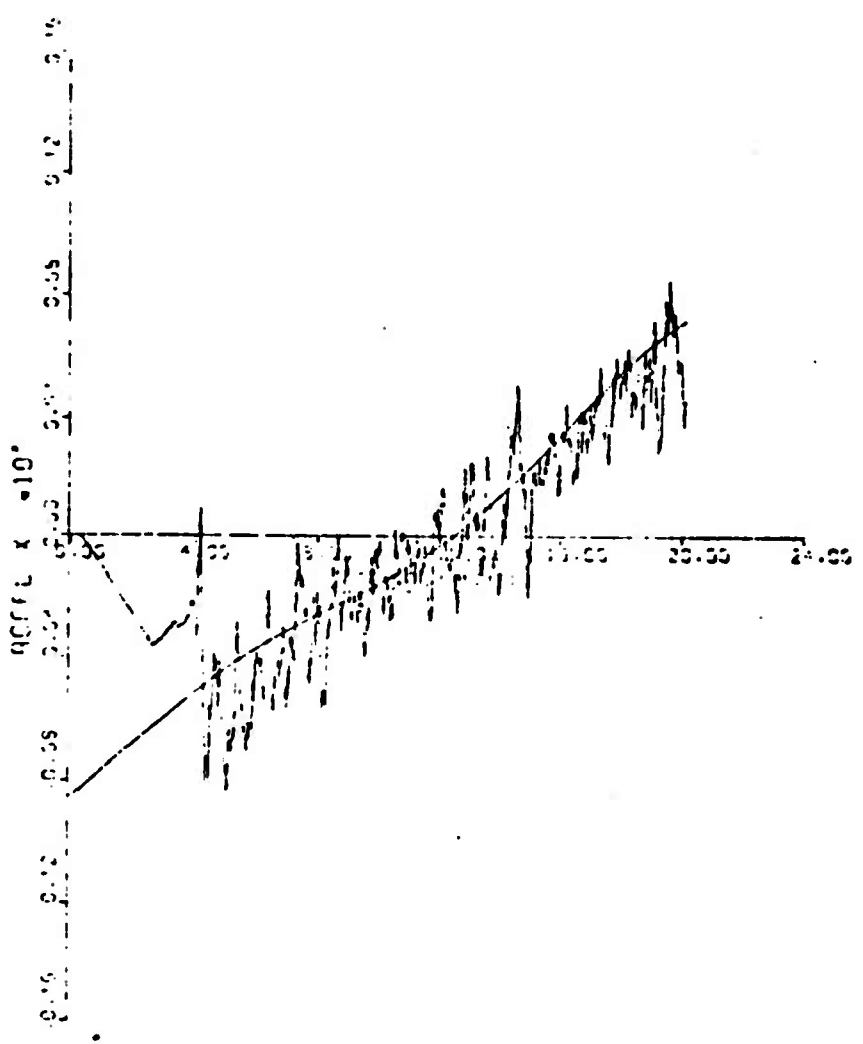

a. X Acceleration (meters/sec$^2$)

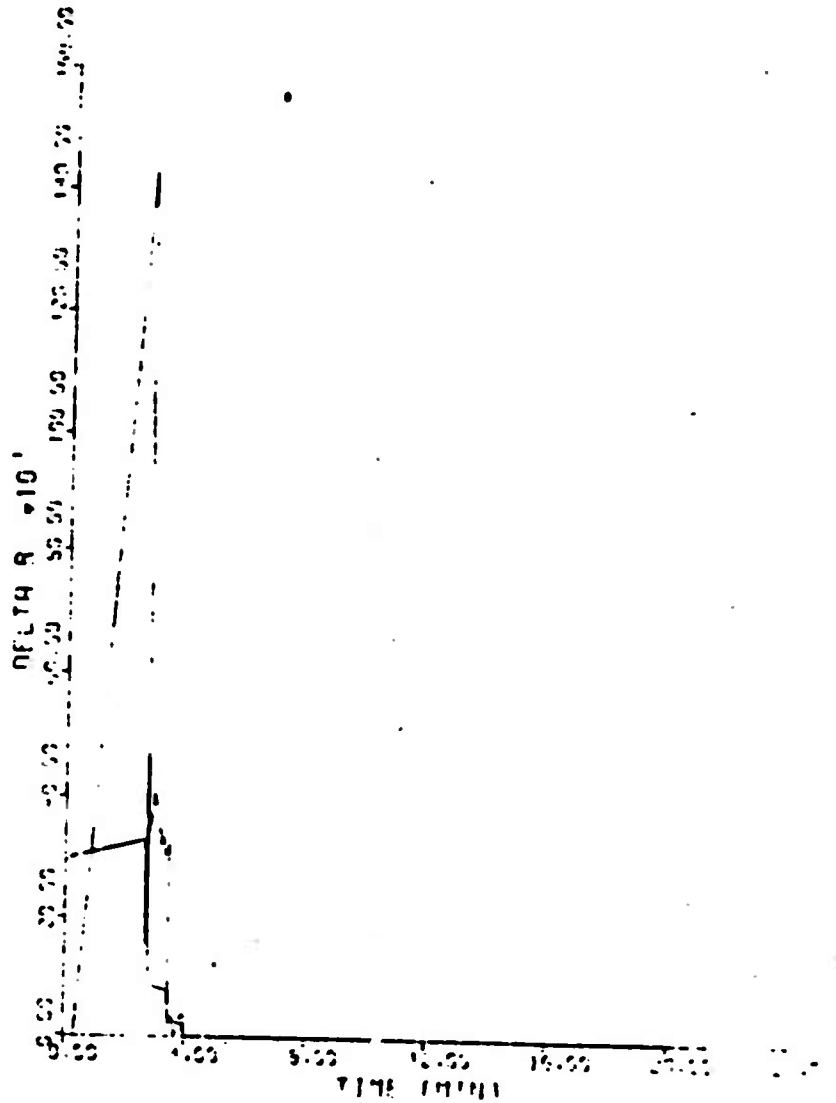

b. Position Error Norm (meters)

Figure 11. Case II Model Error, $\sigma_\rho$ = 1 cm, 25° Elevation Constraint

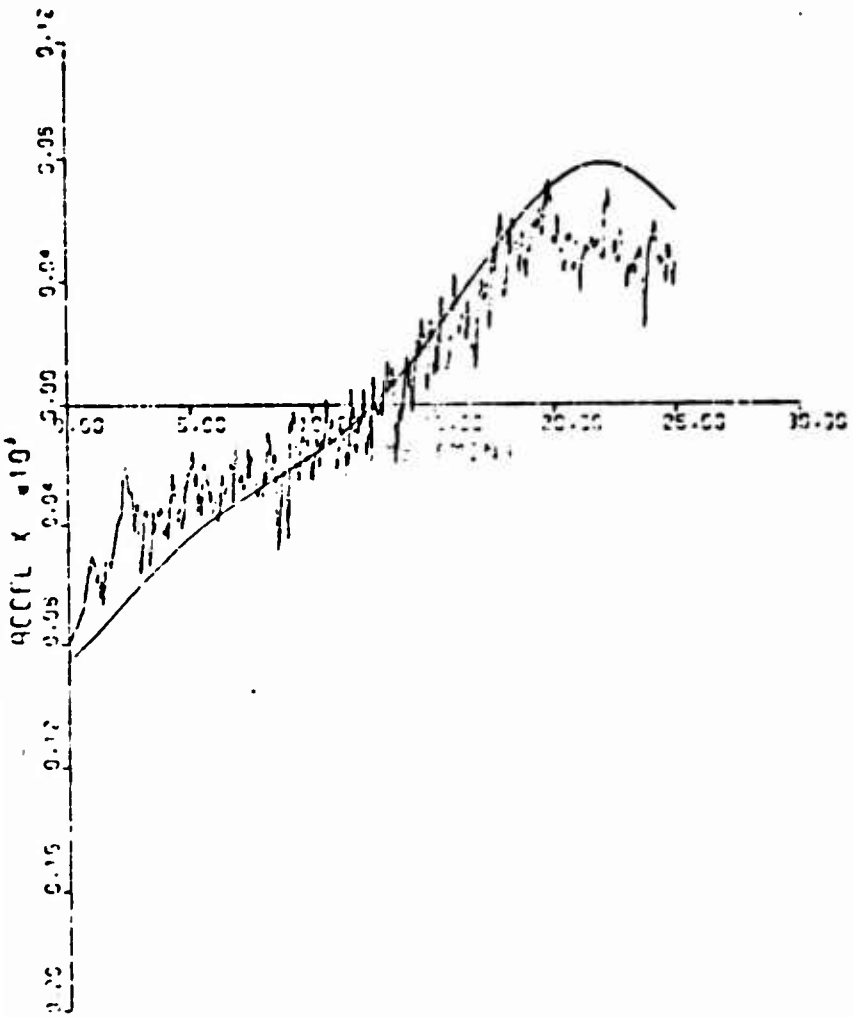

a. X Acceleration (meters/sec$^2$)

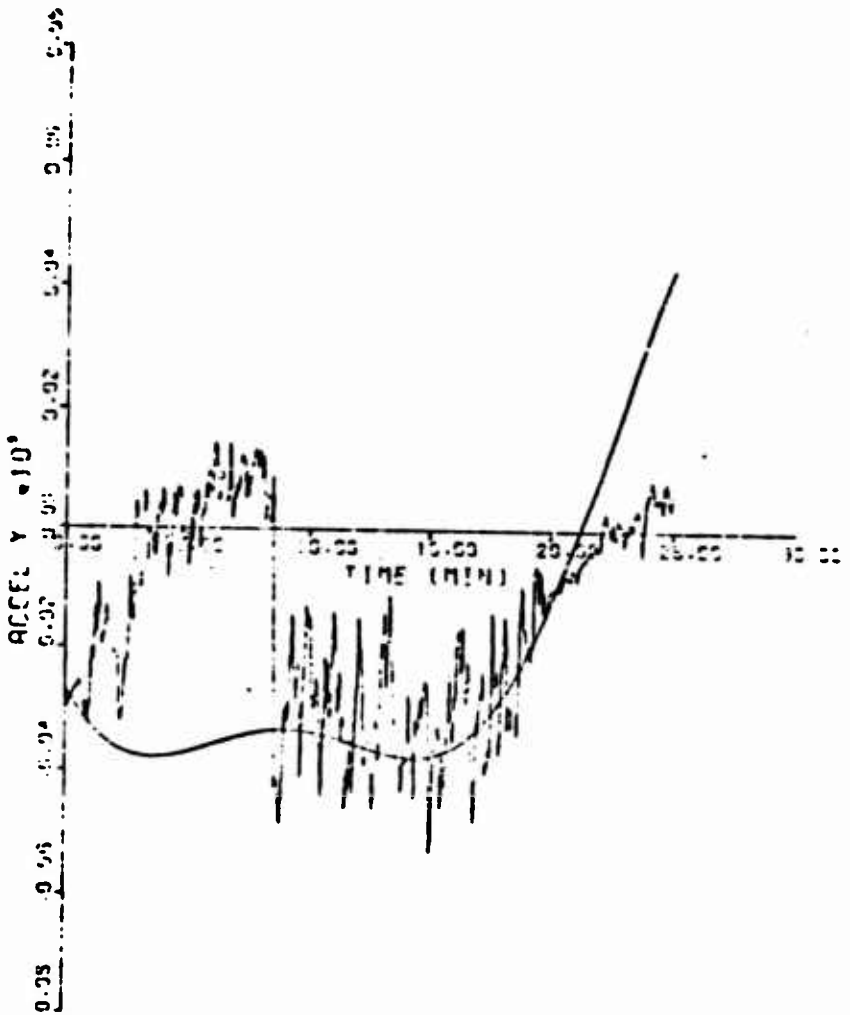


b. Y Acceleration (meters/sec$^2$)

Figure 12. Case II with Three Tracking Stations

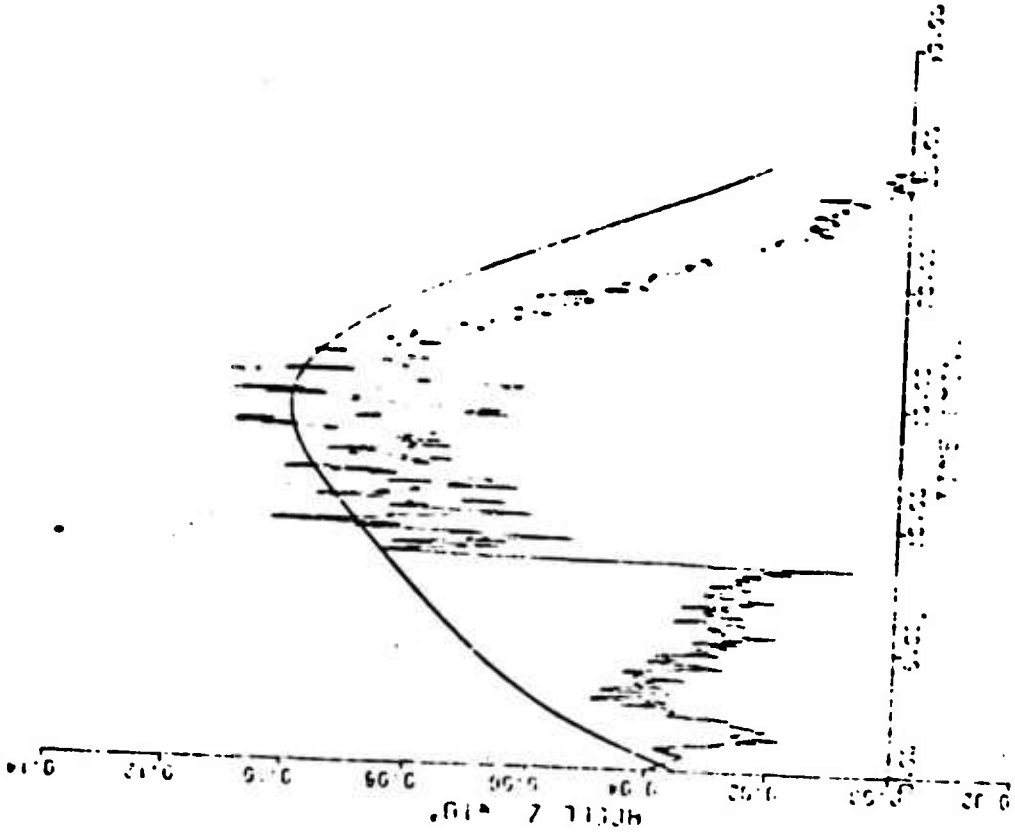

c. Z Acceleration (meters/sec$^2$)

Figure 12 (Cont.)

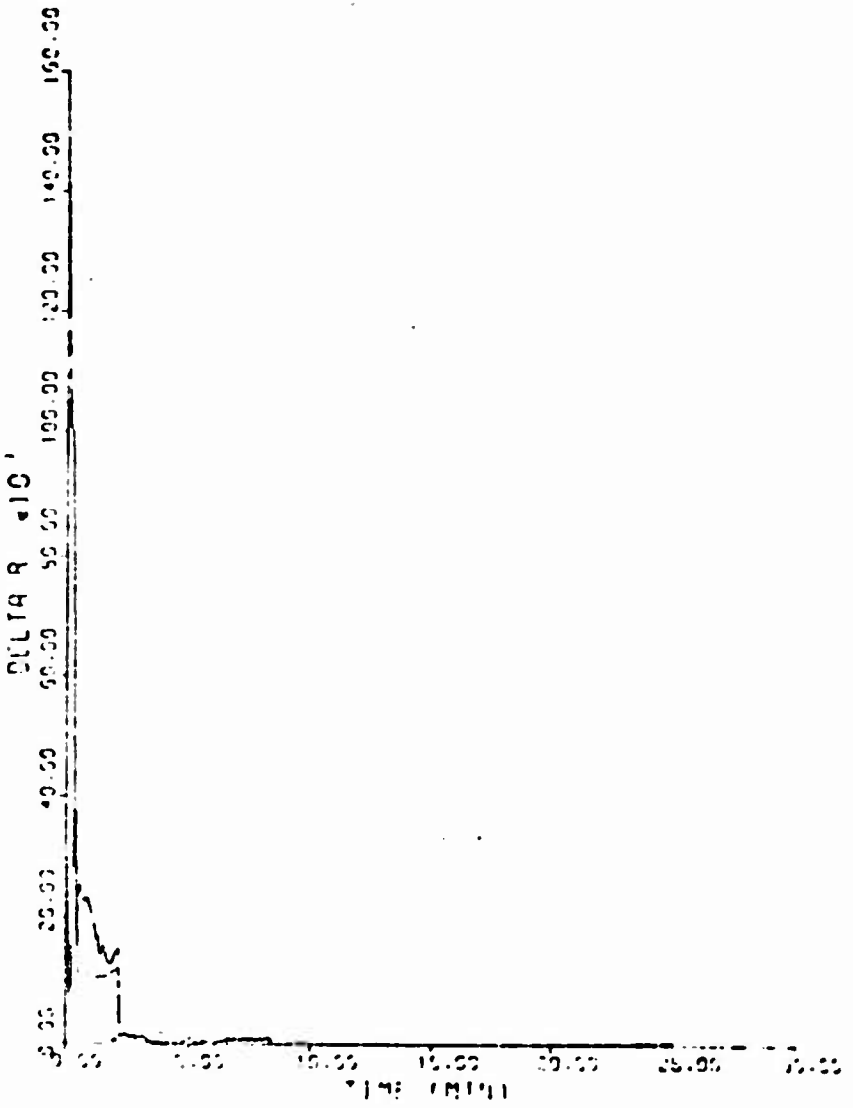

d. Position Error Norm (meters)

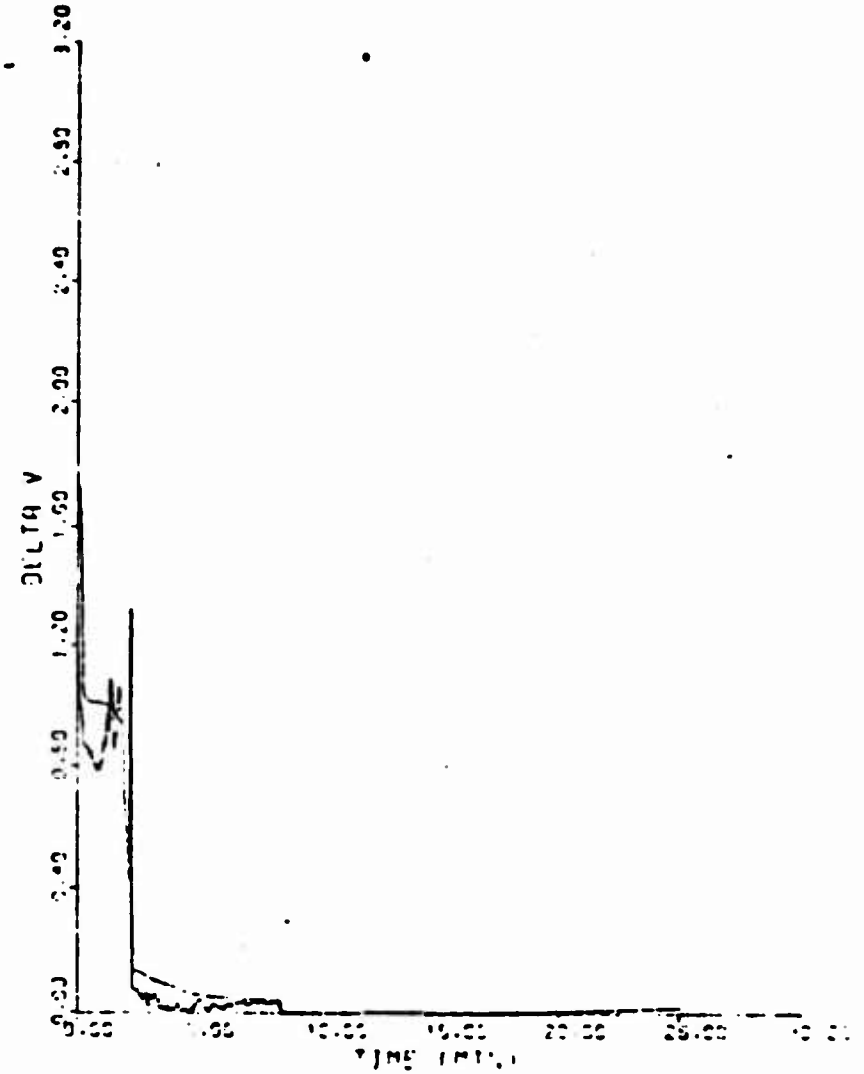

e. Velocity Error Norm (meters/sec)

Figure 19 (Cont.)